

Review

Advances in Methods for Recovery of Ferrous, Alumina, and Silica Nanoparticles from Fly Ash Waste

Virendra Kumar Yadav ^{1,2,*}  and Madhusudan Hiranman Fulekar ^{3,4}

¹ School of Nanosciences, Central University of Gujarat, Gandhinagar, Gujarat 382030, India

² School of Lifesciences, Jaipur National University, Jaipur, Rajasthan 302017, India

³ School of Environment & Sustainable Development, Central University of Gujarat, Gandhinagar, Gujarat 382030, India; mhfulkar@cug.ac.in

⁴ Centre of Research and Development, Parul University, Vadodra, Gujarat-391760, India

* Correspondence: yadava94@gmail.com

Received: 6 April 2020; Accepted: 18 September 2020; Published: 22 September 2020



Abstract: Fly ash or coal fly ash causes major global pollution in the form of solid waste and is classified as a “hazardous waste”, which is a by-product of thermal power plants produced during electricity production. Si, Al, Fe Ca, and Mg alone form more than 85% of the chemical compounds and glasses of most fly ashes. Fly ash has a chemical composition of 70–90%, as well as glasses of ferrous, alumina, silica, and CaO. Therefore, fly ash could act as a reliable and alternative source for ferrous, alumina, and silica. The ferrous fractions can be recovered by a simple magnetic separation method, while alumina and silica can be extracted by chemical or biological approaches. Alumina extraction is possible using both alkali- and acid-based methods, while silica is extracted by strong alkali, such as NaOH. Chemical extraction has a higher yield than the biological approaches, but the bio-based approaches are more environmentally friendly. Fly ash can also be used for the synthesis of zeolites by NaOH treatment of variable types, as fly ash is rich in alumino-silicates. The present review work deals with the recent advances in the field of the recovery and synthesis of ferrous, alumina, and silica micro and nanoparticles from fly ash.

Keywords: fly ash; ferro-alumino-silicate (FAS); alumina; silica; zeolites; ferrous

1. Introduction

Fly ash or coal fly ash (CFA) is a spherical, glass-like, heterogeneous particle produced as a by-product from the combustion of pulverized coal during electricity production in thermal power plants (TPPs). Morphologically, fly ash particles are spherical in shape, with sizes varying from 200 nm to several microns, and structurally have ferrospheres, cenospheres, aluminosilicate spheres, or plerospheres, and irregular-shaped carbonaceous particles [1]. Fly ash has almost all the elements present in geological samples—that is, metals, heavy metals, and organic contents. Though the major composition of fly ash almost remains same throughout the world, the composition still varies based on the source of coal, their geographical origin, furnace temperature, and the operating conditions of the boiler [2]. As fly ash is derived from coal, which is rich in minerals, fly ash is also rich in silica, alumina, and ferrous [3], which are the three major contents of fly ash. Besides this, CFA also has minor oxides, such as rutile, K₂O, CaO, Na₂O, and phosphorous oxides, as well as traces of Cu, Cr, Zn, Ni, and Mo oxides [4]. In addition to this, fly ash is also loaded with several toxic heavy metals, such as Al, Ni, Co, Cr, Cd, Zn, Mo, As, and Hg, which categorizes fly ash into “hazardous materials” [5], and poses a potential threat to the flora, fauna, and the environment.

Every year, a million tonnes (MTs) of fly ash are produced around the globe, especially in the USA, China, France, and India [6]. Fly ash is not a serious concern for developed countries, but it

poses a potential threat for developing countries [7]. This is because the fly ash utilization rate of some of developed countries is more than 90%; for instance, France utilizes almost 100% of fly ash, which indicates complete recycling of the fly ash [2]. At the same time, for a developing country, such as India, the fly ash utilization rate is 50–60%, whereas for other developing countries, it is below 40%. The more aggravating situation is the production of millions of tonnes of fly ash every year around the world. Even in the 20th century, 50% of global fly ash is dumped in the vicinity of TPPs. The dumping of fly ash on fertile agricultural land as landfills deteriorates hundreds of acres of land every year [8], which will ultimately lead to a negative impact on the environment. Moreover, the rainfall on piles of heavy metal-loaded fly ash leads to the leaching of heavy metals into the soil, groundwater, and ultimately rivers and other water bodies [9,10]. This will further lead to water pollution and also poses a potential threat to the aquatic flora and fauna, owing to the increased concentration of heavy metals.

The pollution arising from fly ash might be a negative side, but the presence of valuable minerals (silica, alumina, and ferrous) in higher compositions is the positive side of fly ash [11,12]. As fly ash is derived from coal, which has a high amount of silica, alumina, and ferrous, these elements are also common in the fly ash after combustion [3]. Today, with the continuous advancement of technology and research and development, these fly ashes have found applications in the fields of ceramics and construction, adsorbents, fertilizers, landfills, geopolymers, and metallurgy [9,10]. In ceramics and construction alone, they are used for making fly ash amended cement, tiles, pavement blocks, dike preparation, and embankments, among others [10]. Here, however, we are concerned with the recovery and synthesis of alumina, silica, and ferrous nanoparticles from fly ash. In the last decade, there has been a tremendous revolution in the field of nanotechnology and nanoparticles, which has helped it to find applications in the field of catalysis, drug delivery, medicine, and environmental clean-up [13]. However, as nanotechnology is still in its infancy stage, the synthesis of nanoparticles involves expensive precursor materials and sophisticated instruments, which makes the final nanoparticles very costly. Therefore, the nanotechnology replaces the expensive precursor material with waste materials such as agricultural waste (sugarcane bagasse, rice husk ash, citrus waste) and industrial waste, such as gypsum waste, egg-shell waste [14], red mud, and fly ash. If nanoparticles are synthesized from any of the above-mentioned waste, then the final product will be not only cost-effective, but also eco-friendly thanks to the minimization of the solid waste as pollution.

One such precursor material for the synthesis of silica, alumina, and ferrous nanoparticles is fly ash. Fly ash is a rich source of ferrous (5–15%), silica (40–60%), alumina (20–40%), and calcium (0.5–15%), based on the types of coal used, geographical origin, and operating conditions for the combustion of coal in the thermal power plant [10]. Generally, class F fly ashes are rich sources of ferrous, alumina, and silica, as they are derived from the higher grades of coal—that is, anthracite and bituminous—whereas class C fly ashes have a lower content of ferro-alumino-silicate (FAS), as they are derived from the lower grades of coal—that is, sub-bituminous, lignite, and peat. As silica is present in the highest concentration in all of the fly ashes, most attempts have been made for the synthesis of silica nanoparticles (SiNPs) from various parts of the globe. The most preferred method for the synthesis of SiNPs from fly ash is the alkali dissolution method [15], where the fly ash is treated with 4–16 molarity of sodium hydroxides or potassium hydroxides at a temperature in the range of 90–100 °C for 1–3 h. Another method for silica nanoparticle synthesis is the alkali fusion method [16], where the fly ash is mixed with 4–16 M NaOH or KOH and fusion is done at higher temperatures of 600–1200 °C for 3–8 h in a muffle furnace. The high calcination temperature transforms the inert and crystalline minerals of fly ash into the reactive phase of Al and Si after reacting with sodium and potassium hydroxides [17]. The advantages of such a method is that the new products formed after calcination have high reactivity with acids and bases, which drastically increases the yield of silica. Further, as Al is amphoteric in nature, it can react with both acids and bases, and thus it can be extracted by treating the fly ash with concentrated mineral acids, such as sulphuric acid (H₂SO₄), hydrochloric acid (HCl), and nitric acid (HNO₃), by keeping 4–16 molarity of acids, at temperatures of 100–130 °C for 1–3 h along with

continuous stirring. Besides this, alumina can be extracted from fly ash by treating it with 4–16 M NaOH (keeping the solid-to-liquid ratio 1:5) at 90–100 °C for 1–3 h along with continuous stirring [18]. These procedures do not involve any pretreatment for the elimination of impurities in the form of Fe, Al, Na, Ca, etc., which may contribute, to some extent, to the final synthesized nanoparticles and make them undesirable.

We have reported several pretreatment steps and modifications, in fly ash which has enhanced the yield and purity of the synthesized nanoparticles. We have provided our results, which report that, among all three—i.e., Al, Si and Fe—ferrous should be recovered first, followed by Al and Si. This process minimizes the risk of Fe impurity in the synthesized alumina and SiNPs. The ferrous fractions can be recovered easily by a simple magnetic separation method [19,20] using a strong external neodymium magnet. As fly ash is a mixture of several elements, the extracted ferrous has impurities in the form of Al, Si, Na, K, P, Ca, and carbon, which narrows down its wider application in the industries, especially where purity is a major concern. Here, we have suggested a series of chemical methods for the synthesis of highly pure, single-phase iron oxide nanoparticles (IONPs) from the fly ash extracted ferrous particles. These highly pure IONPs find applications as an adsorbent, environmental cleanup, medicine, drug delivery, magnetic resonance imaging (MRI), etc. [21]. Further, the ferrous free residue rich in silica and alumina could be used as a precursor material for the synthesis of silica and nanoparticles. As alumina is present in inert form, such as mullites in fly ash, it has very little reactivity with acids and bases and most of the alumina remains unreacted [22]. Hence, the recovery or synthesis of alumina with acids make the residue material more suitable for the synthesis of SiNPs and the dried residue, which is rich in silicates, can be used for the synthesis of highly pure SiNPs. As ferrous and Al has been already removed, there is a minimized risk of impurity in the form of Al and Fe in the final product. In the end, the non-reacted, aluminates and silicates are present as the final element in the residue. By optimizing the synthesis conditions, the final Al and Si-rich residue can be transformed into useable and non-hazardous zeolites [23]. From the above section, we may conclude that fly ash can be used for the recovery of ferrous, alumina and silica and consequently help in the minimization of the global solid waste. Additionally, the recovery of value-added minerals from fly ash makes the approach eco-friendly and economical as the raw material is a waste [24].

The present review work is mainly divided into two sections where the first section deals with the detailed physical, chemical, and morphological properties of fly ash, while the second section deals with the advancement in the methods or techniques for the recovery of ferrous, alumina, and silica from fly ash waste. Moreover, in the second section, we have reported all the important landmarks achieved in the field of recovery of ferrous, alumina and silica and their subsequent conversion or synthesis into their respective micro and nanoparticles. From all the earlier reported work, it was found that most of the work dealt with the recovery of one or up to two minerals from fly ash. None of the earlier reported work focused on the recovery of all the three minerals—i.e., ferrous, alumina and silica from fly ash. Additionally, none of these works reported the fate of final fly ash residual material left after the extraction of ferrous, alumina and silica, as it becomes highly reactive after NaOH treatment or silica extraction, which may pose a potential threat to the environment after disposal. Hence, after the recovery of all the steps, we have shown advancement in the recovery of all the three minerals with respect to their yield and purity and also dealt with the fate of the final fly ash residue. We have suggested the transformation of final alkaline reactive residue into a harmless and useable zeolite material by altering the parameters. Thus, the current review highlights the work advancement in the recovery of ferrous, alumina and silica and their subsequent conversion into nanoparticles of high yield and purity.

2. Properties and Applications of Fly Ash

2.1. Morphological Properties of Fly Ash

Fly ash is a sphere-shaped, micron-sized (0.01–100 μ) heterogeneous material, having depositions of mainly Al, Si, Fe and C in variable compositions on its surface, and closely resembles the volcanic ashes [25]. The fly ash particles can be either rough or smooth surfaced based on the type of depositions on their surface. Figure 1 show a typical fly ash particle, which is spherical in shape, whose sizes vary from 0.2 microns to several microns (6 μ). Morphologically, fly ash particles may have differently shaped particles, which also vary in their elemental composition viz. ferrospheres (ferrous rich spherical particles) [26], cenospheres or alumino-silicate spheres [27] (Al- and Si-rich particles), plerospheres [28] (larger spherical particles encapsulate smaller particles), plerospheres, and carbon nanomaterial [10]—i.e., soots, buck balls [29], fullerenes [30,31] and unburned carbon, including both organic and inorganic [2]. Figure 1a,b show fly ash plerospheres, which are thick- and thin-walled. Both the plerospheres have trapped numerous smaller sized spherical particles, along with gases and minerals. While Figure 1c depicts cenospheres which are spherical in shape, having mainly Al and Si, along with carbon, on their surface, Figure 1d shows ferrospheres, which have depositions of ferrous on their surface, due to which they have magnetic properties. The ferrospheres have rough surfaced and dendritic shape on their surface. In comparison to ferrospheres, cenospheres are lighter in weight [32] and have high mechanical strength, thermal resistance and have fireproof property [33]. The globular shape of such microspheres is due to the precipitation of crystalline phases during the cooling of iron aluminosilicate melt drops of complex composition [34]. The crystallite size and the composition of the iron-containing phases, that governs the magnetic properties of the microspheres, depend on both the melt composition and the thermal conditions of microsphere formation [35]. Cenospheres are more dominant structures in the fly ash [32], followed by the ferrospheres, which are spherical-shaped ferrous-rich particles, whose sizes fall in the micron range. The ferrospheres have high depositions of ferrous or Fe, which could be either rough, smooth, elliptical or molten drop-shaped, which are given in Section 4. Besides cenospheres and ferrospheres there is the third type of micron-sized spherical-shaped particles, called plerospheres, which are less frequent in fly ash in comparison to the other two forms. These plerospheres encapsulate several small fly ash particles, minerals and gases inside them during the formation from the molten slag at high temperature in the furnace [36,37]. Additionally, there are a large number of carbonaceous nanomaterials, such as fullerenes, graphene, soots and unburned irregular-shaped carbon particles in fly ash, formed due to the combustion of organic and inorganic carbon minerals present in the coal [38]. Such irregular or angular-shaped carbon-rich particles are shown in Figure 2, taken through Scanning Electron Micrograph (SEM), while the bright colored particles are electron-rich Fe, Al and Si rich region [39].

2.2. Elemental Properties of Fly Ash

The mineralogy and composition of fly ash is not constant, rather it varies from place to place, parent coal source, operating parameters and temperature of TPPs [42], the extent of coal preparation and cleaning, furnace design, usual climate storage [43] and handling. The mineralogical properties determine the crystalline phases of the fly ash, and their composition varies from 15–45% in the fly ash. Generally, fly ash has silica 40–60%, alumina 20–40% and ferrous 5–15% by weight fractions [44], and its composition is shown in Table 1. Almost all the fly ash has mullite, quartz, magnetite, hematite and calcite as the common crystalline minerals [45]. Based on mineral composition and sources of coal, fly ash is categorized into two classes—class F and class C. The major differences between these two classes of fly ash are described here. The source of class F fly ash is anthracite and bituminous coal, whereas for class C it is younger lignite and sub-bituminous coal. The lime content in class F is less than 20%, while class C has more than 20% of it. Ca in class F is mainly present in the form of $\text{Ca}(\text{OH})_2$, CaSO_4 and glassy components, which is 1–12%, and in class C it is 30–40%. Class C has larger amount of crystalline content—i.e., 25–45%—than the class F, which has only 15–45% of the

carbon [9,46,47]. The class F fly ash has a higher amount of alkali and sulfate than the class C fly ash. While, for cementing agent, class F requires Portland cement, hydrated lime and quicklime, whereas class C has self-cementing properties. Class F generally requires an addition of air entrainer, which is not required by the class C fly ash. When it comes to the application, class F is used in high SO_4^{3-} exposure conditions, has high fly ash content concrete mixes and is explored for the structural and HP concretes. Whereas class C fly ash is not suitable for high sulfate conditions, limited to low fly ash content concrete mixes are mainly used for the residential construction.

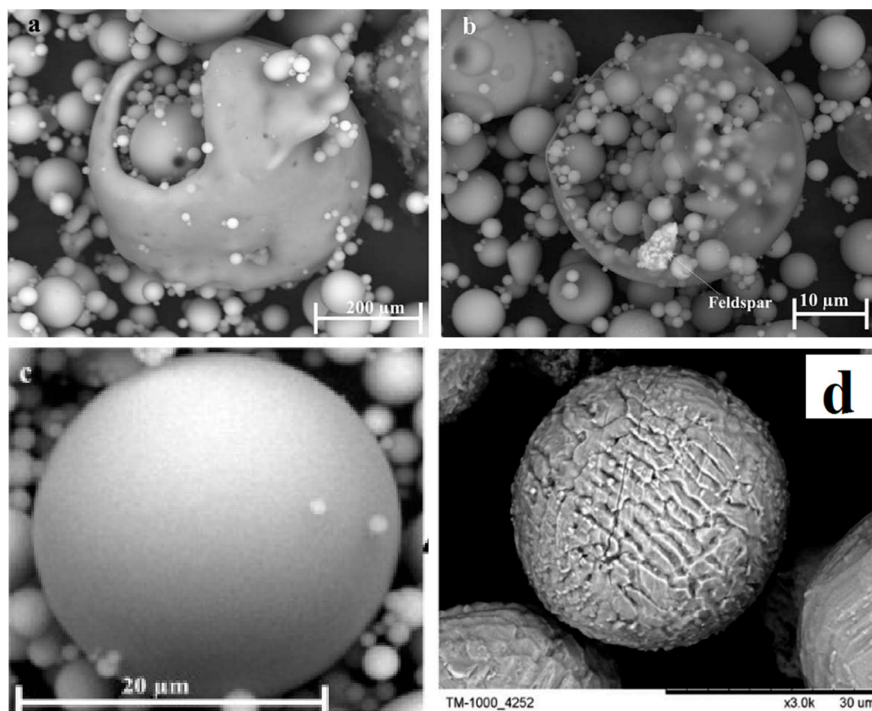


Figure 1. SEM micrograph of fly ash, plerospheres (a,b) cenospheres (c) ferrospheres (d) adapted from Goodzari and Sanei [40] and Olga Sharonova et al. [40].

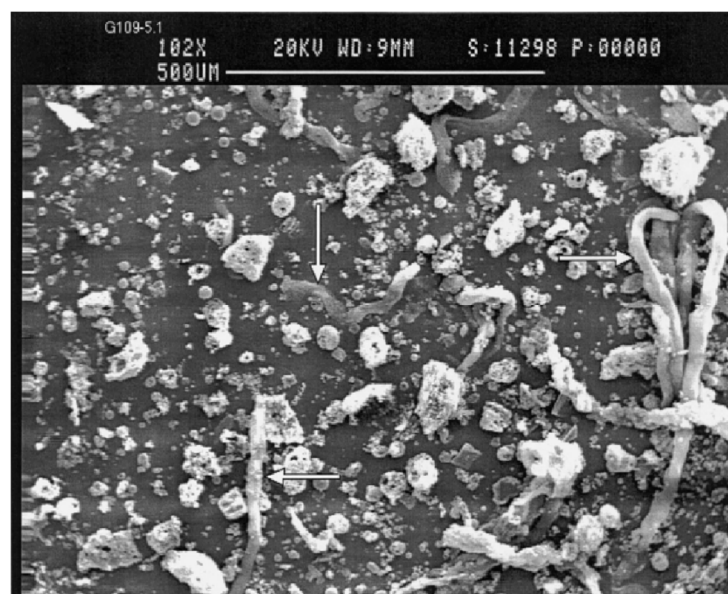


Figure 2. SEM micrograph of fly ash carbon rich particles adapted from Veranth et al. [41].

2.3. Chemical Properties of Fly Ash

The pH of the fly ash tends to vary from acidic to alkaline (4.5 to 12.0), depending on the source of coal and the number of trace elements in them [48]. Fly ash produced from bituminous coal, is mostly acidic even though it has higher sulfur content, while alkaline fly ash is produced from the sub-bituminous coal, which has lower sulfur content, and has higher Ca and Mg content than that derived from bituminous coal [49]. Similarly the electrical conductivity (EC) of fly ash varies between 0.177 to 14 S/m, which directly corresponds to the quantitative concentration of soluble cations and anions in the fly ash [2,50]. Likewise, mineralogy and chemical composition too depend on the various parameters of coal combustion. Chemically, about 90–99% of the fly ash fraction constitutes oxides of silicon, aluminum, iron, calcium and titanium, (~0.5% to 3.5%), which are made up of oxides of sodium, potassium, phosphorus, manganese and sulfur [51], and the remaining fractions are the trace elements, including rare earth and radioactive elements. As per the universal rule, smaller particles with higher surface areas than the larger ones are also applicable to the fly ash particles—hence, smaller fly ash particles tend to accumulate a higher concentration of elements (As, Cd, Cu, Ga, Mo, Pb, S, Sb, Se, Ti and Zn) on their surface in comparison to the larger fly ash particles [52]. Fly ash particles have both crystalline and glassy amorphous materials. Silicates are present in crystalline form—i.e., sillimanite and mullite, while most of the silicates are present in the glass form. The average glass content in U.S. fly ash is 90%, while in Indian fly ash it varies from 49–69% by weight. This indicates that Indian fly ash has more crystalline content than the U.S. fly ash.

Table 1. Normal range of fly ash chemical composition produced from different coal types (in wt. %) [7,53,54].

Components	Bituminous	Subbituminous	Lignite
SiO ₂ %	20–60	40–60	15–45
Al ₂ O ₃ %	5–35	20–30	10–25
Fe ₂ O ₃ %	10–40	4–10	4–15
CaO%	1–12	5–30	15–40
MgO%	0–5	1–6	3–10
SO ₃ %	0–4	0–2	0–10
Na ₂ O%	0–4	0–2	0–6
K ₂ O%	0–3	0–4	0–4
Loss on ignition (LOI) %	0–15	0–3	0–5

The chemical composition of the core or interior part of the fly ash is almost masked by the depositions of elements on the surface layer of fly ash particles [2]. Moreover, these surface layers get depositions of various elements during volatilization and condensation of molten slag in the furnace [55]. It has been reported that the concentration of some of the elements on the surface layer has many more folds than that of parent coal [56]. All fly ashes derived from different coal types, have oxides of Fe, Al, Si and varying carbon content. The chemical composition of fly ashes derived from different coal sources is given above in Table 1.

2.4. Physical Properties of Fly Ash

Based on the percentage of unburned carbon, fly ash color may vary from tan to grey or black [7]. The darker the color of fly ash, the higher the carbon content [57]. Based on the above fact, it is obvious that lower grades of coal (lignite, sub-bituminous) having a lesser amount of carbon, will produce light—i.e., tan to buff-colored fly ash [58]—while the higher grades of coal (anthracite and bituminous), being rich in carbon, will produce dark colored fly ash—i.e., grey to black. Moreover, calcium oxide content too contributes in the color of fly ash, as lower grades of coal have higher calcium content than the higher grades of coal, and provide white shade to the fly ash [55]. The specific surface area and the specific gravity of fly ash tend to vary in the range of 2000 to 6800 cm² per gram and 2.1 to 3.0 g/cm³,

respectively [9]. Regarding the particle sizes of fly ash, their composition varies from one geographical area to other, and for instance, the size of sandy particles is 2–0.5 mm and 4.75–0.075 mm in the U.S. and Indian fly ash, respectively, while the size of silt particles in U. S. fly ash vary from 0.05–0.002 mm and 0.075–0.002 mm in Indian fly ashes. However, the size of clay particles in both U.S. and Indian fly ashes are less than 0.002 mm. Sandy particles in U.S. fly ash are sub-divided into very coarse, coarse, medium, fine and very fine, and their total composition in fly ash is 32.4%, whereas in Indian, fly ash total composition of sandy particles is 35.69%, which indicates that the Indian fly ashes have 2–4% more sandy particles than the U.S. fly ashes. The percentage of silty particles in both U.S. fly and Indian fly ash are more than 60%; however, the U.S. fly ash have marginally higher content of silty particles than the Indian fly ash. The average silty content in U.S. Fly ash is 63.2%, whereas in Indian fly ash it is 62.39%. Clay particles in U.S. fly ash are 4.3% in comparison to Indian fly ash having 1.91% of the clay. Hence, the U.S. fly ash has a 2–3% higher amount of clay particles than the Indian fly ash [7]. Variation in fly ash is also seen due to the different structural properties of the particles—i.e., cenospheres [59,60], plerospheres [61], ferrospheres [62] and irregular- or angular-shaped carbon particles [63], which are already briefly described in the introduction section. Cenospheres have a bulk density in the range of 0.4–0.6 ton/m³ and constitute up to 5% of the total weight of fly ash [32].

2.5. Applications of Fly Ash

Fly ash has great importance and numerous advantages either in the bulk form or in their separate natural nanostructured particles, which is depicted in the Figure 3. Besides, the fly ash also has a higher amount of Si, Al, and Fe that can be used in hydrometallurgy using the environmentally-friendly approach for the recovery of minerals at an economical cost [64,65]. The bulk form of fly ash can be potentially used as a biofertilizer, as it contains a rich source of plant nutrients such as, Na, Ca, K, P, Zn, Mg, Mn, Mo, etc. Moreover, the zeolites synthesized from fly ash can also be used for the sustained and controlled release of the N, P, K and other minerals to the plants [23,66]. In the field of agriculture, [67,68] the bulk fly ash can be used for resource conservation, reclamation of the contaminated sites and restoration of industrial sites [69]. Besides agriculture, the fly ash also finds application in civil engineering [70] (bricks, tiles, cements, blocks), tiles [71,72], brick making, cements, geopolymers [73], landfills [74], mining [75], agriculture river embankments [76], fillers [77,78], panels and composite materials [79] and in metallurgy for the recovery of value-added minerals. The natural nanostructured form of fly ash—i.e., cenospheres, ferrospheres, carbonaceous particles and plerospheres, finds applications in nano-ceramics, mechanical engineering, construction of lightweight materials [80] and wastewater treatment. Besides, individual microspheres are also used for making thermoset plastics, concrete materials, nylon, material for coating [81], high-density polyethylene (HDPE), and others. In, hydrometallurgy, the high content of ferrous, alumina and silica in the fly ash, which is a waste, can possibly be considered as one of the most reliable materials for the recovery of ferrous, alumina and silica and their derivatives [82]. There are several reports where fly ash has been used for the synthesis of highly pure alumina and SiNPs, which are discussed below in Section 4. The recovery of such value-added minerals opens new horizons, as it not only reduces the global pollution in the form of solid waste but also acts as an alternative material for Si, aluminum and ferrous [83].

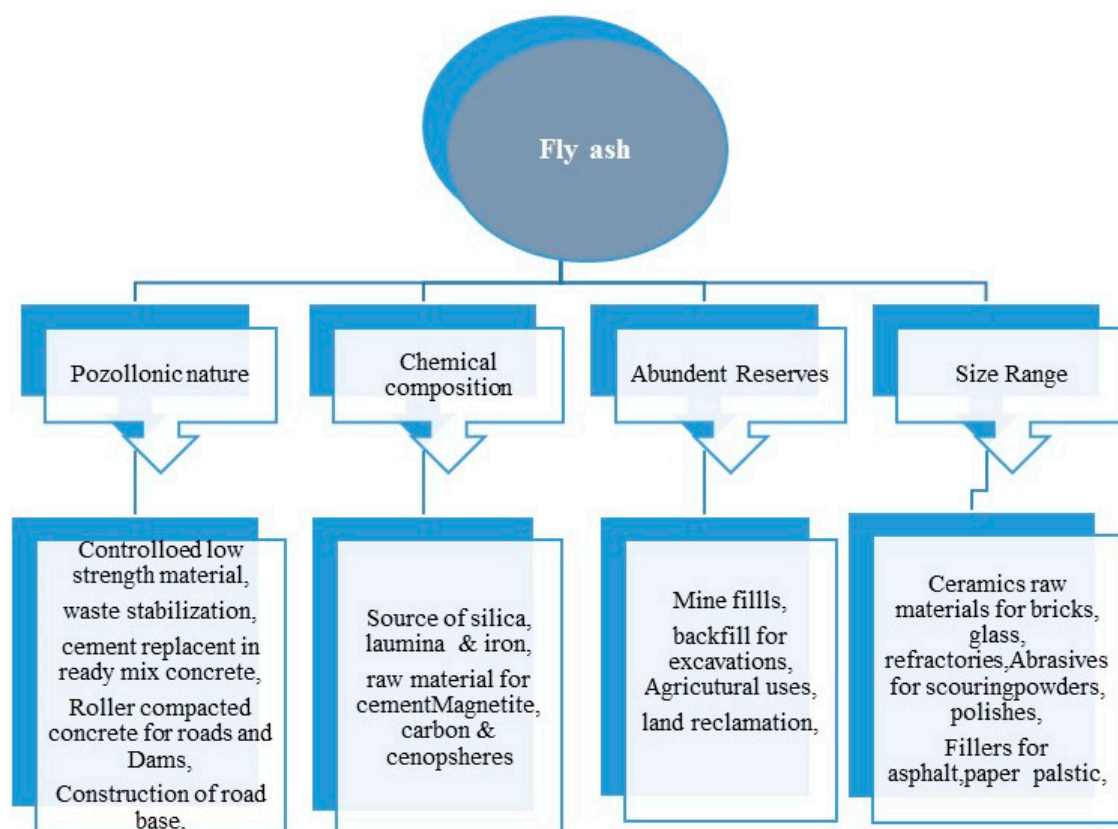


Figure 3. Broad areas of fly ash applications.

3. Fly Ash Production and Utilization at a Glance in India

The major fly ash-producing countries are the USA, China, India, Russia [84] and, out of these, most of the developed countries have started the ~100% utilization of fly ash in the forms of cement, bricks, tiles [85], roads, embankments, etc. [6]. Nevertheless, fly ash utilization has become a major challenge for developing countries, which have a long way to go in order to achieve this effort. Thermal power stations that use pulverized coal/lignite as a fuel produce a huge amount of fly ash as a by-product [86]. In a developing country such as India, fly ash utilization was only 40–60% in the year 2017–2018, and the remaining was disposed in the fly ash ponds that, again, pose a serious threat to the living organism and the environment. In India, during 2016–2017, the total fly ash generated was about 169.25 MTs and, out of which, about 107.10 MTs was utilized, and the remaining 63 MTs was disposed nearby the TPPs [7]. By the end of 2017, there were about 155 thermal power plants that used 600 MTs of coal producing 170 MTs of fly ash and out of which 107 MTs of fly ash was used in different forms by the various industries [7]. This value increased in 2018, where the total TPPs reached to 167 generating an enormous amount of fly ash. In the year 2019, 129 MTs of fly ash was generated, out of which 70% of the fly ash was utilized and the remaining 30% was dumped in the local vicinity of the TPPs. In comparison to several European countries and the U.S.A, India is lagging in fly ash utilization, as these countries have achieved up to 100% utilization of fly ash. Moreover, India still needs a lot of time for the implementation of bulk utilization of the ash. Despite conducting various research studies and the development of numerous technologies for fly ash utilization and proper disposal, a consistent visible trend for utilization has not been obtained. Hence, fly ash management is likely to remain an important area of national concern.

4. Fly Ash as a Source of Ferrous, Alumina and Silica

Although the qualitative compositions of fly ash generated in different parts of the globe are almost identical, they differ in their chemical and physical properties [87]. The utilization of major

fly ash fractions such as magnetic and non-magnetic (alumina and silica-rich) and several other narrow fractions can significantly increase the scope of the utilization of the fly ash from the thermal power plant [88]. However, almost all the fly ash, irrespective of their origin, has almost all the above-mentioned minerals in variable amounts. Based on the mineralogy of fly ash, it can be a reliable and valuable alternative resource for the generation of ferrous, alumina and silica-based micro and nanoparticles [23]. Ferrous, alumina and silica generally co-exist in the fly ash (shown in Figure 4) as either ferro-alumino-silicates (FAS) or alumina, and silica can be present in the form of crystalline mullite, sillimanite or quartz [89,90]. No doubt, fly ash is a rich source of FAS, CaO and rutile (TiO_2), which is primarily composed of amorphous alumino-silicates and other crystalline minerals such as mullite, quartz, hematite and magnetite [91]. The recovery of ferrous particles from fly ash is possible by a simple magnetic separation method, while the residual nonmagnetic fractions rich in alumino-silicates can be used for the recovery of alumina and silica. Once the ferrous fractions are separated from fly ash, then the silica and alumina can be recovered by multidisciplinary approaches—i.e., chemical route (sol-gel) [92], chemical coprecipitation [93], fungal synthesis and bacterial synthesis [94]. The alumina, being amphoteric in nature, can be extracted from the fly ash by chemical approaches such as acidic treatment and NaOH treatment [95]. It can be further converted to nano-alumina powders by several chemical methods, such as thermal decomposition [96], co-precipitation. The major fractions of fly ash are silica that can be extracted by both chemical (NaOH or KOH treatment) and microbial (bacterial and fungal) approaches [4].

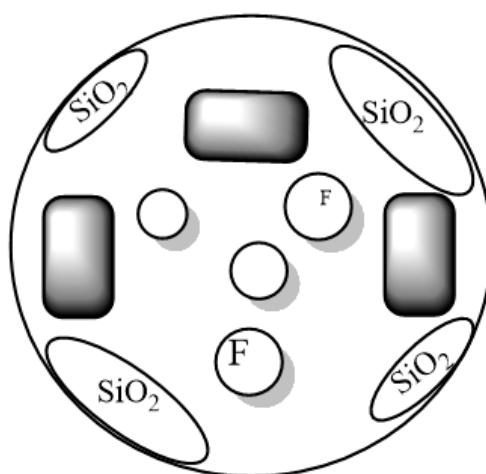


Figure 4. Schematic fly ash particle showing major components on their surface.

Silica is extracted from the fly ash in the form of sodium silicate using chemical methods. Further sodium silicate leachate can be neutralized with dilute HCl, and silica gel can be formed by the sol-gel method [97]. After extracting ferrous fractions, one can extract alumina and silica as the residue is rich in crystalline alumino-silicates that are unreacted and non-extractable. It can be processed and modified further for the synthesis of different classes of zeolites. Ultimately, fly ash may serve as an important alternative material for the recovery of FAS and zeolites [97], which would consequently reduce global pollution in the form of solid waste.

5. Ferrous Particles: Properties and Advances in Their Recovery Process from Fly Ash

5.1. Properties of Ferrous Particles Extracted from Fly Ash

Iron is one of the major elements present in the earth crust and is found in all the earthy materials such as rocks, soils, clay, volcanic ash and coal. The major fractions of iron in coal are present either as sulfur-bearing or non-sulphur-bearing minerals [98]. The sulphur-containing iron minerals in coal are pyrite (FeS_2) [99], jarosite [$\text{KFe}_3(\text{SO}_4)_2(\text{OH})_6$] [100], troilite [101] and pyrrhotite [102] (both FeS) [103,104],

while the non sulphur-bearing iron minerals [105] are ankerite ($\text{CaFe}(\text{CO}_3)_2$) [106–108], illite [109] and siderite (FeCO_3) [110–112]. The generation of ferrospheres occurs in the carbon matrix, which provides a reducing medium when iron-containing minerals from coal interact with other elements of coal in the molten form and transform into ferrous oxides. These ferrous oxides are, especially, magnetite, hematite and maghemite, along with Al, Si, Ca, etc. [62,113]. The extraction and utilization of ferrous materials from waste fly ash not only makes the whole process greener but, at the same time, it also reduces the burden from the environment in the form of pollution. The fly ash extracted ferrous particles are mainly spherical in shape, along with few elliptical, molten-drop, dendritic-shaped particles [55]. The deposition of ferrous particles is responsible for the magnetic properties of ferrospheres. The deposited ferrous particles are either angular or spherules shaped. The deposited iron oxide phases vary from magnetite, maghemite, hematite and goethite. The Fe is always associated with other elements, such as Ca, Al, Si, Ca, Mg, Na, O, P, etc., and ferrous particles are always associated with elemental oxides of these elements, and find applications in iron-based industries, which are described below in detail, under Section 6.1.

5.2. Advances in the Recovery of Ferrous Particles from Fly Ash

The ferrous particles extracted from fly ash can be used as the precursor material for the synthesis of various types of pure IONPs [114]. Moreover, they also act as an alternative source for different iron oxide-based industries [115], such as steel and steel-based industries. Conventionally, ferrous particles are extracted either by wet magnetic separation method or by dry magnetic separation method [116]. Both the methods apply an external magnetic field, but one is extracted in the slurry form, while the other is extracted in their dried form, as shown in Figure 5. In the dry form, it can be extracted by using conveyor belts with a magnetic effect at one end, while in wet slurry it can be extracted by using a strong external magnet [82]. There have been several advances in the extraction of ferrous particles from fly ash in the last three decades and these are highlighted here in chronological order.

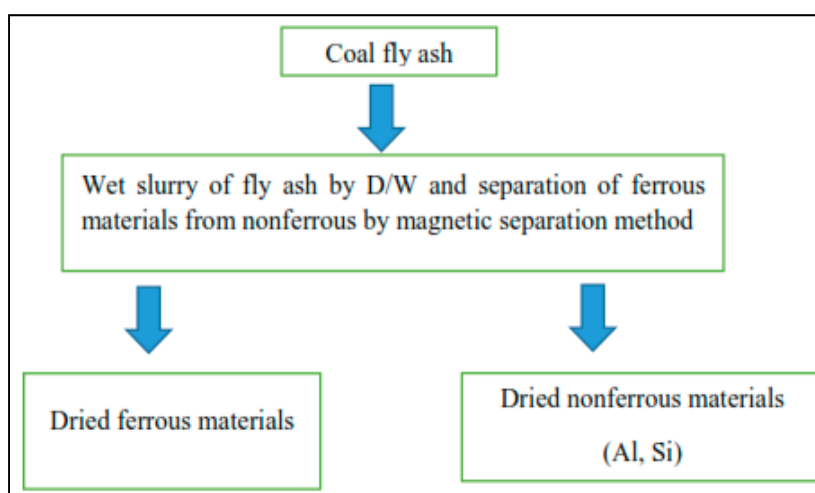


Figure 5. Schematic diagram for magnetic separation of fly ash ferrous fractions.

Olga et al. [117] isolated and studied the composition and morphology of the magnetic microspheres from two different fly ash samples from Russian thermal power plants. About eight fractions of ferrospheres in a range of sizes from 0.4 to 0.02 mm were recovered from high-calcium fly ash and studied using the scanning electron microscope—Electron diffraction spectroscopy (SEM-EDS) analysis of ferrospheres and ferrospheres composition. Shoumkova et al. [118] reported the physicochemical characterization and magnetic separation of coal fly ashes from the various regions of Russian TPPs [119]. The fly ash magnetic concentrates were isolated by wet high gradient magnetic separation using a laboratory-scale solenoid separator of SALA type. Besides this, they also studied

the comparative properties of magnetic and non-magnetic fractions. Xue and Lu, [120] studied the microstructures of ferrospheres in fly ashes with their detailed SEM, Energy Dispersive X-Ray (EDX) and Environmental Scanning electron microscope (ESEM) analyses. Here, the magnetic ferrospheres were isolated by magnetic separation technique and the various phases found in the fly ash were magnetite and hematite. The extracted ferrospheres contained Al, Si, S and Ca and were reported as having morphological structures in the form of smooth, polygonal, dendritic, granular and molten drop characteristics. Oliveira et al. [121] reported the extraction and characterization of spinel magnetites from the silico-aluminous fly ash from TPPs of a French region using SEM-EDS, X-ray Diffraction (XRD), TEM, Mossbauer spectroscopy and Variable sample magnetometer (VSM). It was concluded that Mg substituted Fe in the magnetite structure and the formula was closer to $MgFe_2O_4$ than Fe_3O_4 . Apart from this, there was Mn, Ca and Si at lower percentages. Fomenko et al. carried out the phase composition of magnetic microspheres isolated from Russian TPP and performed a Mossbauer study in six narrow size ranges of magnetic microspheres isolated from power plant fly ash. It was found that Al, Mg and Ti are the major phases in the isolated magnetic microspheres. They reported that the magnetic properties of magnetic microspheres depend on the Fe content and the distribution pattern of the cation over the spinel sites [122]. Fulekar and Yadav [50] extracted ferrous particles from the fly ash slurry using an external magnet in conjunction with an ultrasonicator, where slurry was fed to the ultrasonicator fitted with a strong neodymium magnet. The sonication causes the lysis of larger particles into several smaller particles, which in turn releases the trapped ferrous particles, and consequently has an enhanced effect on the recovery of ferrous particles. It was further purified by stirring on a magnetic stirrer without using a magnetic bead. The ferrous particles respond to the magnetic field of the stirrer where ferrous particles adhere to the center, while non-ferrous particles adhere at the periphery of the Petri plate. Finally, the dried ferrous particles were analyzed using UV-Visible spectroscopy, Fourier transform infrared spectroscopy (FTIR), VSM, dynamic light scattering (DLS), particle size analysis (PSA), XRD, Field Emission Scanning electron microscopy (FESEM) and TEM. The analyses revealed that the particles were spherical in shape, whose sizes varied from 200 nm to 7 microns, and had mixtures of different iron oxide phases. Fulekar and Yadav [50] treated ferrospheres with acid and used the ferrous rich solution to synthesize ferrous carbonate, maghemite, magnetite and hematite of high purity at nanoscale, using a chemical precipitation and calcination method by optimizing environmental parameters. The purity of transformed IONPs varied from 93–97% [50]. Further, the synthesized IONPs were used for the heavy metal removal from fly ash-based simulated wastewater.

From the above-mentioned work it can be concluded that, to date, investigators have only recovered ferrous fractions from fly ash by applying either wet magnetic separation or dry separation methods. Further, almost all of them have characterized the extracted ferrous fractions from fly ash by using FTIR, VSM, DLS, PSA, XRD, FESEM and TEM. The investigators concluded that the extracted ferrous particles are rich in Fe, and spherical-shaped ferrospheres have either rough or smooth surfaces. Rough surfaced ferrospheres are due to the deposition of large spherules or angular deposition on the surface of preformed cenospheres, whereas the smooth-surfaced ferrospheres have even distribution of ferrous on their surface. The shape of the deposited iron oxide particles on the aluminosilicate spheres are angular, rectangular, and mostly present in the mixed phases of hematite, magnetite and maghemite. Rough surfaced ferrospheres have a strong magnetic property in comparison to the smooth-surfaced ferrospheres. Smooth-surfaced ferrospheres have fewer depositions of ferrous particles on their surface so they have weak magnetic properties. Besides rough and smooth-surfaced ferrospheres, there were few of elliptical, molten-drop, or dendritic shape [55].

From, all the reported works, it was found that Fe was always associated with other elements, such as Ca, Al, Si, Ca, Mg, Na, O, P, etc. [39], and hence the ferrospheres were never free from such elemental oxides. Such impure fly ash ferrospheres have been used as fillers in nanocomposites, coke, smelting [12], steel production and other iron and iron-based industries [123]. Additionally, the ferrospheres also find their application in catalysis—i.e., for profound oxidation and oxidative

coupling of methane (OCM) [124], thermolysis of heavy oil and petroleum residue [114], magnetic carriers for the separation of recombinant proteins [125], and composite sorbents.

Specifically, it was shown that small amounts of ferrospheres containing 87.5% Fe₂O₃ and 2.0 wt. % MnO are catalysts for the oxidative coupling of methane [126], while narrow fractions of ferrospheres with a lower iron content are effective catalysts for the CH₄ deep oxidation [127,128]. The purified ferrous particles can be applied in the field of in medicine and drug delivery—i.e., in MRI, radionuclide therapy, medical diagnosis, cancer-hyperthermia, magnetic storage, magnetic ink printing, a biosensors and for bioseparation for portable devices [21].

Thus, here in our ferrous recovery we have reported a method for the elimination of elemental impurities from ferrospheres by acidic treatment—i.e., concentrated HCl treatment of ferrospheres in 1:20 ratio, under sonication at 70–80 °C for one hour. Further, the ferrous rich acidic leachate was used for the synthesis of four different types of IONPs (ferrous carbonate, magnetite, hematite and maghemite) under optimized conditions. The purity of such single phased IONPs varied from 86–97% and their purity was cross-checked with the commercially available nanoparticles in the market. This method has suggested the transformation of ferrous particles into highly pure IONPs. The summarized tabulated form of various ferrous recovery approaches is highlighted below in Table 2.

Table 2. Ferrous fractions, their properties, and extraction from fly ash.

Authors	Ferrous Particles	Instruments	Impurities and Findings
Gomes et al. [129]	Magnetite	Scanning Electron Microscope-Electron Diffraction Spectroscopy (SEM-EDS), X-ray Diffraction (XRD), Transmission Electron Microscope (TEM), Mossbauer spectroscopy and Vibrating sample magnetometer (VSM)	Mg has substituted Fe in the spinel structure
Bayukov et al. [35]		Mossbauer spectroscopy	Al, Mg and Ti were the major phases
Shoumkova et al. [118]			Studied the comparative properties of magnetic and non-magnetic fractions
Olga et al. [40]		SEM-EDS	Ferrospheres of sizes 0.4 to 0.02 mm were recovered from high-calcium fly ash, SEM-EDS study
Feng and Gao [120]	Magnetite and hematite	SEM-EDX and ESEM analysis	Studied the microstructures of ferrospheres in fly ashes with their detailed SEM, EDX and ESEM analysis.
Yadav and Fulekar [130]	Magnetite and hematite	TEM, Fourier transform infrared (FTIR) and Particle Size Analyzer (PSA)	Reported the nanosized, magnetic particles in class F fly ash from Gandhinagar, Gujarat, India.
Fulekar and Yadav [50]	Magnetite, hematite	TEM, XRD, SEM-EDS, Raman, FTIR, VSM, PSA	Studied the morphological, elemental and mineralogical properties of class F fly ash
Fulekar and Yadav [50]	Synthesized: Ferrous carbonate, Magnetite, Hematite, magnetite	TEM, XRD, SEM-EDS, Raman, FTIR, PSA	Synthesized ferrous carbonate, magnetite, maghemite and hematite by using extracted ferrous particles with high purity.

6. Extraction and Synthesis of Alumina Nanoparticles from Fly Ash

Aluminum is the third largest element in the earth crust, and is a constituent of soil, rocks and minerals, such as bauxites and clay. Aluminum, being amphoteric in nature [131], can leach out from the source material either by strong alkali hydroxides or strong mineral acids. Generally, aluminum is present in the crystalline form, such as alumina in fly ash [132]. Mullite is one such mineral in fly ash, which has a high composition of alumina [133]. Mullites are mostly present in the matrix part of fly ash [134,135], which makes it a very difficult task to leach out alumina in higher concentrations into the solution. Until now, numerous investigators have successfully extracted the alumina by means of both acidic treatment and NaOH treatment. High-alumina coal fly ash is a potential starting material for the preparation of $\text{Al}(\text{OH})_3$ [136]. Techniques of the aluminum extraction from coal fly ash can be classified into acidic [136], alkali [136] and acidic–alkali method [137,138]. The acidic method requires acid-resistant and airtight processing equipment. The acidic–alkali method is a complicated process [24] with a series of procedures [136], including sintering [139], silica–alumina separation, purification [140], precipitation [141,142] etc. The alkali dissolution method is a promising method for avoiding calcinations of the coal fly ash at a higher temperature (more than 800 °C) and lower energy cost [136,143]. Several investigators previously reported alumina extraction methods, out of which a few of them are described below.

6.1. Alkali-Based Extraction

Park et al. reported that the synthesis of alumina from fly ash derived highly pure alum using $\text{NH}_2\text{Al}(\text{SO}_4)_2$ [96]. It was achieved by mixing CFA with ammonia in the water at controlled pH followed by the successive crystallization. The effect of heating (conventional and microwave) was observed on the decomposition of the alum. Alumina extracted from the microwave-assisted-derived alum was a fine powder with a high surface area. Fly ash-based ultrafine $\text{Al}(\text{OH})_3$ was synthesized by the NaOH dissolution method by Su, Yang [138]. It was reported that silica was extracted by 8 M NaOH at 90–95 °C for 150 min and the extraction efficiency of silica was 40%. In the next step, alumina was extracted at 260 °C for 60 min by mixing fly ash with white lime and 20 M NaOH. The alumina extraction efficiency was about 89% and the final product was aluminum hydroxide instead of alumina, which can be further converted into alumina by calcination at a high temperature. Li et al. extracted Al_2O_3 from fly ash by the mixed-alkaline hydrothermal process [137]. Here, alumina leaching was done using a solution of NaOH and calcium hydroxides by a hydrothermal process, and further alumina leaching in accordance with temperature, solid to liquid ratio and Ca/Si ratio was observed. The Ca effect on the alumina leaching was seen with increased temperature, calcium-silicon ratio and solid-liquid ratio. Under optimal conditions, alumina extraction reached to 91.3%. Wang et al. reported a technique “ NH_4HSO_4 roasting technology” for the recovery of aluminum and iron from fly ash [144]. It is a two-step procedure, wherein Al and Fe were leached out from fly ash and the leached Al, and Fe were precipitated with the NH_4HCO_3 solution. Again, it was leached with a NaOH solution, and finally there was the carbonation-based decomposition of the $\text{NaAl}(\text{OH})_4$ solution. Hence, it is a novel method for the extraction of alumina from fly ash. The study comprised of thermodynamics and kinetics of Al recovery from fly ash and reported Al extraction efficiency up to 90.5% by optimizing conditions at CFA: ammonium hydrogen sulfate, 1:8 mole at 400 °C for 60 min.

Virendra Yadav [50] reported a method where the fly ash was added to concentrated sulphuric acid of 2–8 M, (but most preferably at 8 M) by keeping a solid–liquid ratio of 1:5 in a 100–200-mL round-bottom flask in a reflux condenser. The reaction was carried out for 60–90 min at 90–260 °C with continuous stirring at 400–500 rpm. After the completion of the reaction, the leachate was collected by centrifugation at 5000–7000 rpm for 5–10 min. The alumina leachate obtained in the form of aluminum sulfate was directly calcinated in a muffle furnace at 800 °C for 6 h in a quartz crucible. The properties of the synthesized nanoparticles were analyzed by sophisticated instruments, such as FTIR, Raman, PSA, XRD, FESEM and TEM. Further, the ferrous-free fly ash, was separately mixed with 8 M concentrated sulphuric acid, nitric acid and hydrochloric acids by maintaining a solid–liquid ratio of 1:5 at 125 °C

with continuous stirring at 400–500 rpm for 90 min in a 100-mL round-bottom flask fitted with a reflux condenser. All three acids were analyzed for their leaching efficiency of Al. It can be concluded that HCl had maximum leaching efficiency. Further, the alumina leachate was converted directly to solid alumina by calcination at 600–700 °C for 56 h in a quartz crucible. The summarized form of extraction of Al and synthesis of alumina and its derivatives by alkali-based dissolution from fly ash are given below in Table 3.

Table 3. Acid-based dissolution of Alumina from fly ash.

Authors/ References	Operating Conditions	Leaching Agent	Product	Findings	Efficiency %
Park et al. [145]	CFA with ammonia in water at controlled pH followed by successive crystallization	$\text{NH}_4\text{Al}(\text{SO}_4)_2$	Alumina/alum	Alumina derived from the microwave assisted derived alum was finer powder with a high surface area	-
Su, S. et al.; Su, Yang [136]	Alkali-dissolution process		Ultrafine aluminum hydroxide	2 steps: (1) Silica extraction by NaOH by 8 M for 150 min at 90–95 °C, efficiency 40%; (2) Second alumina extraction at 260 °C for 60 min by mixing fly ash + white lime + 20 M NaOH	~89%
Huiquan Li et al. [137]	Mixed-alkaline hydrothermal method	Alumina leaching was done by mixed hydroxides of NaOH and $\text{Ca}(\text{OH})_2$ through the hydrothermal methods	Alumina	Al leaching was seen with increased temperature, calcium–silicon ratio and solid–liquid ratio.	91.3% (optimized conditions)
Wang et al. [146]	NH_4HSO_4 Roasting technology		Aluminum hydroxide, Alumina	A two-step procedure in the first step Al and Fe was extracted while in the second step leached Al and Fe was precipitated with NH_4HCO_3 solution	-
Wang et al. [146]	Ammonium hydrogen sulfate roasting technology		Alumina	Studied thermodynamics and kinetics of alumina extraction from fly ash. It was achieved when the CFA: ammonium hydrogen sulfate ratio was 1:8 mole at 673 K for 60 min	90.5% (optimized conditions)

6.2. Acid-Based Extraction

Matjie et al. [138] reported the recovery of Al_2O_3 from bituminous coal-derived fly ash of South African TPPs where the calcium aluminate was obtained by mixing CFA with CaO and then calcinated at 1000–1200 °C. It was further treated with sulphuric acid and about 85% alumina extraction was reported using this approach. Nayak and Panda (2010) reported sulphuric acid-based extraction of alumina from Talcher (Odisha) TPPs fly ash and proposed that lower sulphuric acid molarity and ambient heat is not suitable for the recovery of a higher amount of alumina and the same can be achieved only at a higher solid-to-liquid ratio [147]. Shi et al. prepared coarse alumina nanoparticles from fly ash using sulphuric acid as a leaching agent [148,149] and the extraction efficiency of alumina was 87%. Bai et al. achieved alumina extraction of up to 85% by concentrated sulphuric acid-based thermal decomposition, where calcination at 300 °C converted most of the alumina into aluminum sulfate [150]. Wu et al. reported the leaching of Al from the fly ash using concentrated H_2SO_4 along with pressure. They also reported the effect of coal size, experiment timing and temperature on Al leaching from fly ash. They concluded that pressure and the smaller size of fly ash particles have positive effects on the Al extraction from fly ash. Al extraction efficiency reached up to 82.4% under optimal conditions [151]. Shemi et al. reported several processes for aluminum recovery and, in one of the methods, they used 6M sulphuric acid at 250 °C for 6 h along with acetylacetone in the gas phase for the facilitation of the alumina extraction [152].

From all the above-reported methods for alumina extraction, it was found that sulphuric acid was employed for the leaching of Al or alumina extraction from fly ash. The Al extraction efficiency varied from 82.5% to 92.2%. It was observed that the molarity of acids, base and temperature also play an important role. The high molarity of either acids or base at high temperatures can increase the yield of alumina extraction from the fly ash. Here, Al was extracted using sulphuric, nitric and hydrochloric acids, but alumina was synthesized by only sulphuric acid-treated leachate. The Al leachate obtained was directly converted to alumina powder by the calcination of leachate at a temperature above 600 °C. The summarized form of extraction of Al and synthesis of alumina and its derivatives from fly ash by the acid-based treatment method is given below in Table 4.

Table 4. Alumina extraction from fly ash by acid-based method.

Authors/References	Operating Conditions	Leaching Agent	Product	Findings
Matjie et al. [138]	Mixing CFA with CaO and then calcinated at 1000–1200 °C	CaO, sulphuric acid	First calcium aluminate, Second alumina	Firstly, calcium aluminate was produced, further treated with sulphuric acid, and ~85% Al was extracted
Nayak and Panda 2010 [147]	Sulphuric acid based extraction of alumina and leaching behaviors from the fly ash collected	Sulphuric acid	Alumina	Reported: Not possible to get high recovery of alumina by direct acid leaching at low acid concentration and ambient temperature. Higher extraction of alumina is possible only at a higher solid: liquid ratio. Leaching of metals also depends on the nature of leaching medium, solid: liquid ratio, temperature and leaching time.

Table 4. Cont.

Authors/References	Operating Conditions	Leaching Agent	Product	Findings
Shi et al. [149]		Sulphuric acid	Coarse alumina nanoparticles	Al extraction rate-87%
Bai et al. [150]	Thermal decomposition—Fly ash + concentrated sulphuric acid and calcined at 300 °C, due to this, most of alumina is converted to aluminum sulfate	Sulphuric acid	Alumina Aluminum sulfate	Al extraction up to 85%
Wu et al. [151]	concentrated sulphuric acid + along with pressure		Alumina	Reported effect of coal size, reaction time and temperature on the Al leaching from fly ash. Pressure as well as smaller size have positive effects on the Al extraction. Al extraction efficiency was 82.4% under optimal conditions.
Shemi et al. [152]	Al extraction by 6 M sulphuric acid by using acetylacetone in the gas phase. Temp: 250 °C for 6 h for optimum yields	Acetylacetone	Alumina	Application of acetylacetone in gas phase for alumina extraction.
Fulekar and Yadav [50]	Al extraction by 4–8 M using sulphuric acid. Temp: 125 °C for 90 min with stirring	Sulphuric acid	Alumina, Aluminum sulfate Aluminum hydroxides	Aluminum extraction was 40%. Obtained mixtures of alumina, aluminum sulfate and aluminum hydroxides with low Al content—i.e., below 15%.

6.3. Acid-Alkali Based Extraction

Several studies report the use of both acidic and alkaline treatment applied subsequently in order to increase the yield of alumina leachate and ultimately the extraction of alumina particles from fly ash. Aluminum, being amphoteric in nature, dissolves in both acids and bases, but the extraction of Al with strong mineral acids alone is not that effective as the alumina (mullite and sillimanite) in fly ash is mainly crystalline and inert. Both of these sources of alumina can readily react with a strong alkali, such as NaOH. The application of both the strong acids and bases along with heating may facilitate the conversion of the retractile, crystalline and inert material to react and ultimately make them available into the solution. To date only a countable number of attempts have been made in this field, which necessitates further extensive research work.

Valeev et al. reported a method where Al-chloride solution obtained by leaching coal fly ash can be further processed to extract sandy grade alumina, which is essentially suitable for metallic aluminum production. They reported the formation of amorphous alumina via the calcination of aluminum chloride hexahydrate obtained by salting-out from acidic Al-Cl liquor. This step was followed by the alkali treatment with further Al₂O₃ dissolution and recrystallization as Al(OH)₃ particles, and a final calcination step was employed to obtain sandy grade alumina with minimum

impurities. The major advantage of this novel approach is that the process does not require expensive high-pressure equipment and also reutilizes the alkaline liquor and gibbsite particles from the Bayer process, which significantly reduces the production cost of the sandy grade alumina [153].

6.4. Microbial Leaching of Alumina from Fly Ash

Certain fungi and bacteria have a capability of Al or aluminum leaching from bauxite, fly ash, kaolin and red mud, as they produce several mineral and organic acids along with numerous carbohydrates, which has been reported earlier by numerous investigators. Bacteria, such as *Thiobacillus spp*s [154], *Acidithiobacillus* bacteria [155–157] sulfate reducing bacteria (SRB) [158] and others, produce dilute sulphuric acid, that acts as an extractant for the aluminum and other metals from fly ash and other similar sources of alumina. As acids are produced in milli mols quantities, the Al leaching efficiency with these bacteria is not as effective as it is with the chemical method.

While fungi, such as *Aspergillus niger* [159], *Penicillium notatum* [160] and *Penicillium chrysogenum* [161] produce citric acids, gluconic acids and several other weak organic acids that act as the main lixivants for Al leaching from the fly ash. These weak organic acids are also responsible for various metabolic activities in the fungi [162]. *A. niger* is ubiquitous in nature and thrives in the air, soil and indoor environments. The citric acids also take part in the leaching of metals from several metallic samples. *A. niger* strains are used in the industries for the commercial production of citric acids [163]. Previously this strain was used to leach out Al and Fe from the bauxite, kaolin and fly ash, but no attempt has yet been made for the synthesis of alumina. This fungus produces citric acid as a major metabolite in the sucrose growth medium that leaches out alumina and other metals such as Fe. Nevertheless, the yield is very low due to the lower citric acid generation in the medium. Few investigators have used *Penicillium* and *A. niger* for the alumina extraction from bauxite, red mud, kaolin and fly ash [164]. Some of the previous work done in the field of bioleaching and the biosynthesis of alumina is highlighted below.

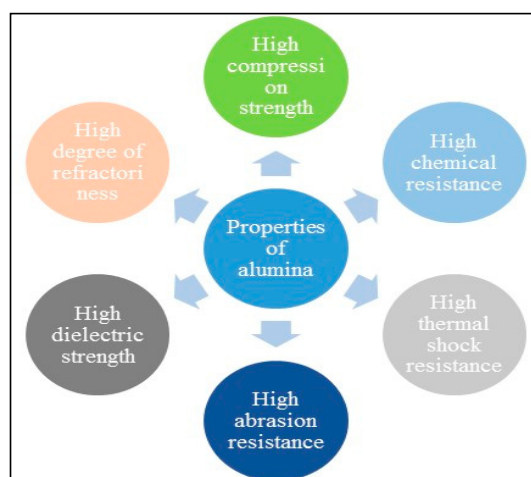
Xu and Ting described the effect of bioleaching on the fly ash by *A. niger* [165]. They conducted a study to find optimal parameters for metal bioleaching by varying fly ash pulp density, spore and sucrose quantity and the timing of fly ash addition [166]. The Al and Fe leaching was reported to be 12.3 ppm, which was far lower than the Zn, which was reported as 77.6 ppm. The acids responsible for the leaching were citric acid and gluconic acid. Again, the same group of investigators in 2009 reported the *A. niger*-based bioleaching of Al, including other metals from fly ash [167]. They showed that the leaching concentration of metals was directly related to citric acid productions. Krishna et al. reported alumina extraction from the bauxite red mud by using numerous extremophiles bacteria [168]. *A. niger* was used for the initial bioleaching of Al from ferrous free fly ash residue and then for the further synthesis of alumina from the leachate. Fulekar and Yadav [50] carried out the Al leaching from fly ash using *Asp. niger* (grown in sucrose medium) supernatant, and wet mycelia in an incubator shaker at 200 rpm and at 28 °C for 48–72 h. Fly ash was mixed with supernatant and 10 g of wet mycelia and the solid-to-liquid ratio 1:5 was maintained. The leachate was obtained by filtration using Whatman filter paper no. 42 under sterile conditions in both of the experiments. The leachate was dried in a rotary evaporator; the obtained powder was analyzed by UV-Vis, PSA and FESEM-EDS. The summarized form of fungi mediated the extraction and synthesis of alumina and its derivatives from fly ash, which are given below in Table 5.

Table 5. Aluminum leaching by from fly ash by fungi.

Authors/References	Operating Conditions	Fungus Used	Product	Findings
Xu and Ting [165]	Citric acid, Gluconic acid	<i>Aspergillus niger</i>	Al in the medium	Reported that the optimal parameters for bioleaching of metals by varying CFA pulp density, spore concentration, sucrose concentration and time of addition of CFA. Leaching of Al and Fe was 12.3 ppm, which was far lower than the Zn, which was 77.6 ppm. The responsible acids for the leaching were citric acid and gluconic acid.
Xu and Ting [166]		<i>Aspergillusniger</i>	Al in the medium	Showed that the leaching concentration of metals was directly related to the citric acid productions.
Fulekar and Yadav [50]	Citric acid	<i>Aspergillus niger</i>	Al, Al ₂ (SO ₄) ₃	Showed that the lesser yield of alumina present in mixtures of alumina, aluminum sulfate and Al(OH) ₃

6.5. Properties and Applications of Alumina Nanoparticles

Alumina occurs in numerous meta-stable phases, which include gamma [γ]-, epsilon [η]-, delta [δ]-, theta [θ], kappa [κ]- and χ-alumina. Among all these phases of alumina, the [α] phase is the most stable, while the gamma phase is the most important and widely used nanosized alumina material. Gamma alumina is widely used in petroleum and automobile industries as a catalyst and catalyst substrate; in ceramics [169] and glasses. It is used as an adsorbent, for spacecraft materials, microelectronics, thermal resistant materials, biomedical purposes [170], as a coating material for thermal wear and abrasive optoelectronics and in metallurgy [171]. Ultrafine aluminum hydroxide is an important green flame retardant inorganic material with multi-functions of retarding, suppressing smoke and filling [172]. The various important properties of alumina and alumina nanoparticles [173–175] are given below in Figure 6. The fly ash based extraction of alumina can be considered as an environmentally-friendly approach and is important from a scientific point of view as it focuses not only on the disposal of waste but also acts as a substitute for aluminum source [138].

**Figure 6.** Properties of alumina nanoparticles.

7. Synthesis of SiNPs from Fly Ash

The synthesis of SiNPs from fly ash has been reported using chemical and biological methods. The chemical methods initially involve the extraction of sodium silicate from the fly ash using strong hydroxides followed by neutralization by sol-gel technique, whereas microbial synthesis has been carried out using *Fusarium oxysporum* under optimized conditions. Both approaches are mentioned below for the recovery and synthesis of SiNPs from fly ash.

7.1. Silica Extraction from Fly Ash by Chemical Method

It is possible to extract silica from fly ash either by alkali-dissolution [176] or by the alkali-fusion method [177]. The alkali-dissolution based silica extraction is done at 90–100 °C, for a duration of 90–150 min with a variable stirring speed and molarity of NaOH, shown in Figure 7. In the alkali dissolution method, the silicates from fly ash react with the NaOH in the aqueous phase to form sodium silicate. Further, the sodium silicate is treated with dilute HCl or sulphuric acid to form a silica gel by sol-gel technique. In the alkali fusion method [178] (shown in Figure 8), fly ash is mixed with NaOH or KOH and calcinated at a higher temperature to obtain a new fused silicate product. Further, the recovery of silicate from the silicate material is done by acidic treatment. However, fly ash has several acid-soluble elements such as Na, K, P, Mg, Ca, and Fe [18,179], which can be present in the obtained silicate in a minute quantity [20].

Therefore, these alkali and other metals can be eliminated by dilute HCl treatment at above 100 °C for 2–3 h. It is a conventional Bayer's process for the silica extraction from the silicate-rich material. Previously, numerous researchers have reported silica extraction from fly ash by alkali-dissolution methods. A few of them are highlighted below in chronological order.

Falayi et al. leached out silica from fly ash by KOH by varying the stirring rpm, size of fly ash, extraction temperature and solid-to-liquid ratio [180]. The optimum extraction parameters include time 6 h; 3M KOH; solid-to-liquid ratio 1:25 temperature 100 °C; rpm 500. However, there was no attempt made for the synthesis of SiNPs from the leachate further. Similar, work was also carried out by Wang et al. who studied the kinetics of silica and alumina extraction from fly ash by concentrated NaOH and observed the effect of temperature, stirring speed and mass ratio of sodium hydroxide to silica, on silica extraction rate [144]. The silica extraction was found to be 95.6% under the optimized conditions. Piekos and Paslawska (1998) investigated the leaching of Si element from fly ash, which was carried using distilled water, seawater and synthetic seawater with variable ratios of water and fly ash [181].

Virendra Yadav (2019) extracted sodium silicate from ferrous free fly ash using 8 M NaOH by keeping the solid-to-liquid ratio at 1:5 at 95 °C for 90 min along with stirring at 400–500 rpm. Silica gel was obtained by neutralization with 1M HCl and, finally, dried powder was treated with 1M HCl at 110 °C for 3 h to remove the trace elements in the form of impurities. The obtained precipitate was initially oven dried at 40–60 °C, followed by calcination at 400 °C for two hours. The purity of the obtained SiNPs was more than 92%, as confirmed by the EDS [50]. Virendra Yadav (2019) reported the synthesis of amorphous SiNPs from Gandhinagar (Gujarat, India), thermal power plant using the alkali dissolution method. The ferrous and alumina extracted fly ash residue was treated with 8 M NaOH, at 95 °C, in a round-bottom flask under reflux systems for 90 min by maintaining a solid-to-liquid ratio of 1:5. The leachate of sodium silicate was obtained by centrifugation at 7000 rpm for 10 min. The residue was discarded while the sodium silicate was used for the synthesis of SiNPs by sol-gel method. Further, about 40 mL of sodium silicate was titrated with dilute 2N HCl at room temperature. A white gel formed near pH 10, which ceased to form on the further addition of dilute HCl. The gel was left undisturbed for 24 h for ageing. Further, the mixture was centrifuged at 5000–7000 rpm for 10 min to obtain the white precipitate. The white precipitate was dried in an oven at 60 °C for 4–6 h and was finally calcinated at 400 °C for 4 h in a muffle furnace by slowly increasing the temperature by 10 °C/minute until the temperature reached 400 °C. The final synthesized SiNPs were characterized using FTIR, PSA, FESEM-EDS, TEM and XRD. It was found that the sizes of SiNPs ranged between

40–80 nm, they were spherical in shape, and were fused together to form a floral-shaped aggregated structure. The SiNPs were amorphous in nature and a broad hump was observed in the 2-theta region at 15–30°, having peaks centered at 21–22°. FTIR also reveals the three characteristic bands of SiNPs in the region of 400–1200 cm^{-1} . The EDS revealed the purity of SiNPs, which was 80–95%, and had impurity in the form of Na, Al and C due to the improper washing of SiNPs [50].

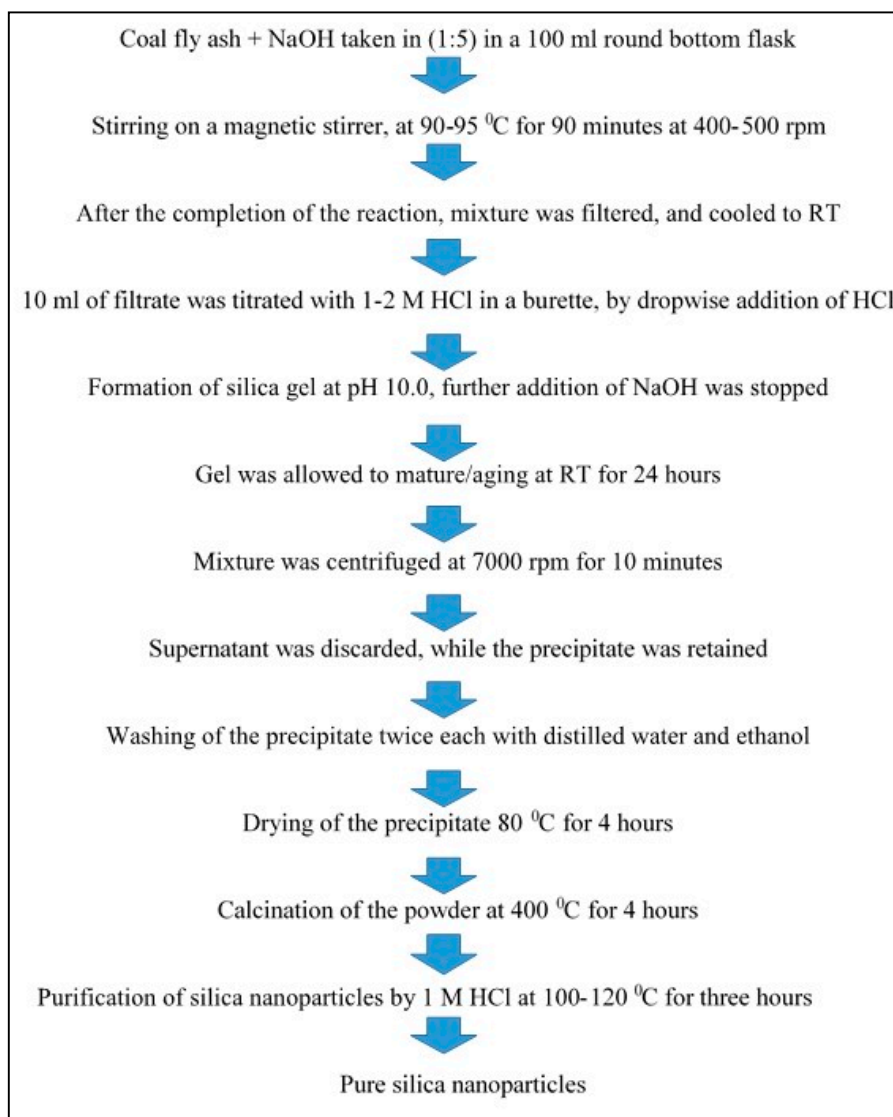


Figure 7. Steps involved in silica synthesis by alkali fusion: chemical method.

Further, Yadav et al. reported the synthesis of SiNPs from the fly ash tiles from Okhla, New Delhi, TPPs. Here the tiles were crushed into powder using a mortar pestle and it was mixed with sodium bicarbonate in the ratio of 1:3 in a platinum crucible and calcinated at 1000 °C for 30 min. After the completion of fusion, the mixture, along with crucible, was dipped in a boiling mixture of dilute HCl and H_2SO_4 in a beaker. Heating was done until the complete dissolution of the lumps. Finally, the mixture was filtered through Whatman filter paper no. 42, where the supernatant was discarded and the solid powder was retained. The filter paper along with the powder was calcinated at 400 °C for two hours. After the analysis of SiNPs by instruments, it was found that the particles were spherical shaped, fused and highly aggregated together to form large particles. The EDS revealed the purity, as there were only peaks for Si and O, mainly along with minor peaks of trace elements. The FTIR revealed the three characteristic bands in the region of 400–1200 cm^{-1} and XRD revealed broad humps with a peak

centered at 2-theta 22° , which confirms the amorphous nature of the SiNPs [182]. The summarized form of the chemically-mediated extraction and synthesis of silica from fly ash are given in Table 6.

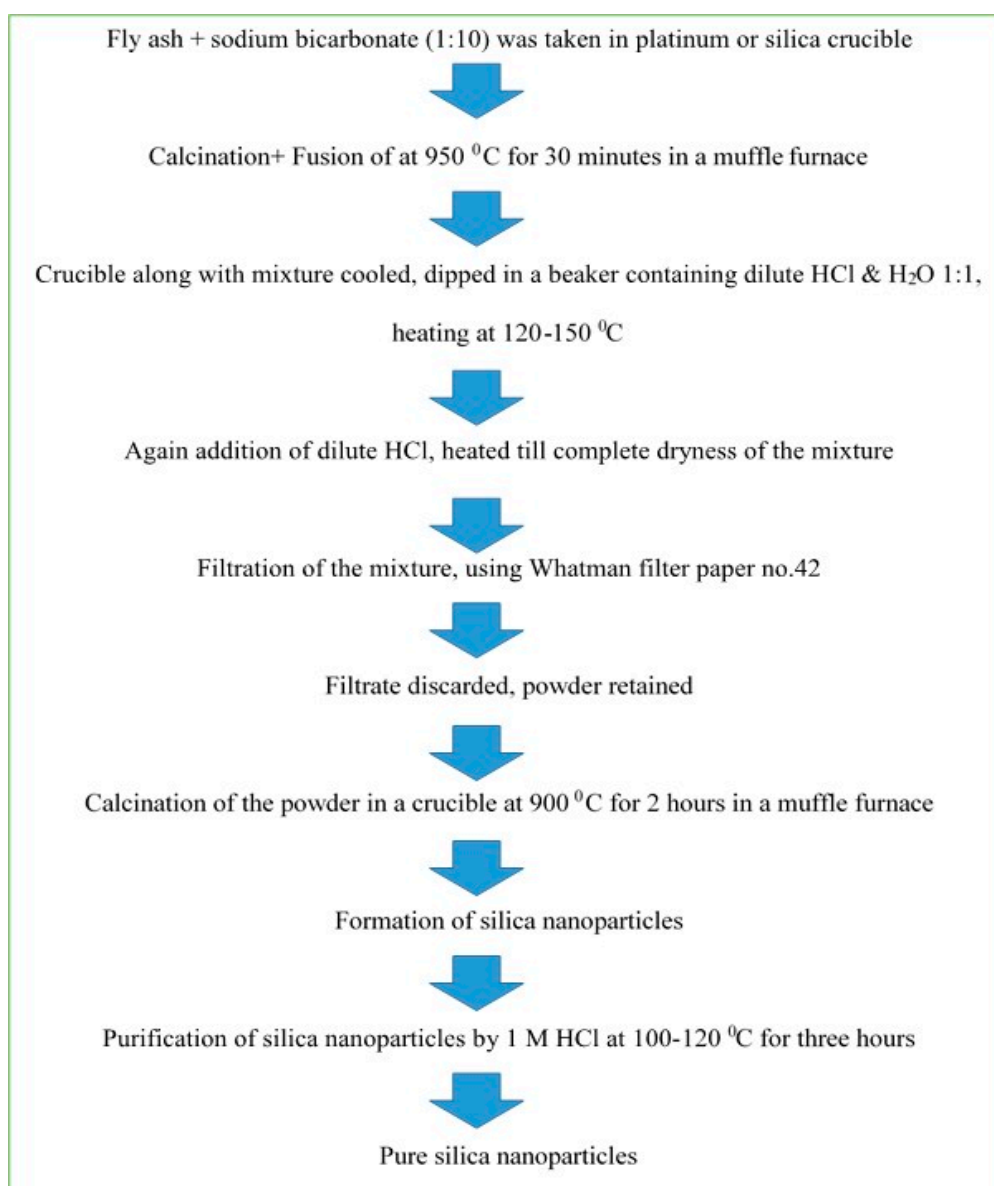


Figure 8. Steps involved in the silica synthesis and purification by chemical method.

Table 6. Silica leaching and synthesis from fly ash by chemical approaches.

Authors/References	Operating Conditions	Leaching Agent	Product	Findings
Falayi et al. [180]	Optimum leaching parameters were time 6 h, Molarity of KOH = 3M, rpm 500, 25 S/L ratio, temperature: 100°C	Leaching of silica by KOH	silica leachate	Found the optimal conditions of silica leaching for time, temperature, molarity of KOH

Table 6. Cont.

Authors/References	Operating Conditions	Leaching Agent	Product	Findings
Wang et al. [144]		Concentrated NaOH		Studied the kinetics of silica and alumina leaching from the extracted slag of fly ash. Studied the effect of leaching temperature, stirring speed and mass ratio of NaOH to SiO ₂ , on silica leaching rate. The silica leaching was 95.6% under the optimized conditions
Piekos and Paslawska [181]		Distilled water, sea water, synthetic sea water with the variable ratios of water and fly ash		Leaching of assimilable silicon species from fly ash
Fulekar and Yadav [50]	Temp: 90–95 °C Time: 90 min Stirring: 300–500 rpm	4–16 M NaOH	Clustered silica nanoparticles	Amorphous, nanosilica, aggregated to form a cluster of size 20–80 nm with 90–97% purity

7.2. Microbial Leaching of Silicon and Silica Syntheses from Fly Ash

Microbial methods can be used for the leaching of silica from the fly ash by fungi and bacteria. These microbes produce different acids, enzymes and other metabolites that initially leach out Si from the fly ash and then transforms the leached Si from the medium into SiNPs. Microbial-based silica synthesis has advantages over chemical methods, as there is no need for toxic chemicals. However, microbial methods are time-consuming in comparison to chemical methods. Bacteria also have a tendency to dissolve the silica from various minerals. A group of bacteria called “Phosphate solubilizing bacteria” [183] has a tendency to leach out silica from the silicates [184]. Bacteria belonging to this group are *Bacillus circulans*, *Bacillus mucilaginous*, *Bacillus edaphics* [185]. These bacteria show a significant effect in mineral solubilization, and are mainly phosphates, as well as silicates in the soil for the proper uptake of the nutrition by the plant. These bacteria have certain enzymes—polysaccharides—that have a valuable role in silica leaching wherein mucopolysaccharide [186] is the main lixiviant for the silica. Previously, Zhan et al. used the three different *Bacillus* strains and studied the leaching of silica from the bauxite ores by individual bacteria as well as in co-operation [187]. The mixed culture leached more silica from the solution in comparison to the individual microbe. Among fungi, only *Fusarium oxysporum* has been used for the synthesis of SiNPs from fly ash, where the purity of silica was up to 40% and impurities in the form of carbon 50% were present [188].

Bacillus circulans is Gram-positive, rod-shaped, endospore-forming bacteria that has the potential to desilicate the silica-enriched media [189]. They are a chemo-organoheterotrophic bacterium that leaches out silica from silicates by attacking the alumino-silicate bonds [190]. It is generally used as a bio-fertilizer as they have a tendency to dissolve the K and Si from soil [191]. They are also called “siliceous bacteria” as they can destroy the silica-rich minerals [192]. These heterotrophic bacteria can grow at temperature, ranging between 5–20 °C or 30–37 °C, but most optimally at 30–37 °C. They produce an extra-cellular polysaccharide, capsular slime and other metabolites such as organic acids 2-Keto gluconic acids, ammonia and various other amino acids which play a role in silica leaching [193]. Silica removal from fly ash by silicate bacteria *B. circulans* is due to the production of mucilaginous capsules containing exopolysaccharides (EPS) [194]. Here, in our approach,

it produces mucopolysaccharides (MPS) that attacks the Na-silicate bonds and leach out soluble silica in the medium.

Virendra Yadav [50] synthesized porous silica nanosheets of size 80–120 nm by using *B. circulans* MTCC 6811 supernatant and fly ash-extracted sodium silicate. The silica was synthesized after the incubation of the fungal supernatant and sodium silicate mixture at optimized conditions. The optimum ratio was 4:1 of supernatant to the extracted sodium silicate by volume. Fulekar and Yadav synthesized spherical shaped aggregated clusters of SiNPs of size 40–80 nm by incubating the *Fusarium oxysporum* supernatant and sodium silicate at optimized ratio—i.e., 3:2 in an incubator shaker at 28 °C for 48–72 h [50]. Here the Si was leached from the sillimanite and mullite of fly ash by the hydrolytic enzymes of *F. oxysporum*. The leached Si from the fly ash forms water-soluble SiNPs which was further dried and silica powder was obtained using the rotary evaporator. Khan et al. [188] also reported the leaching of Si from these two minerals of fly ash and the formation of water-soluble SiNPs which were recovered using the rotary evaporator. The summarized form of fungi-mediated leaching and synthesis of silica/silicon from fly ash are given below in Table 7.

Reactions:

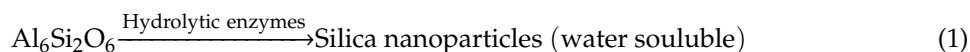


Table 7. Microbial leaching of silica and synthesis of SiNPs from fly ash.

Authors	Operating Conditions	Leaching Agent	Product	Findings
Zhan et al. [187]		Muco-polysaccharides	Soluble silica in the medium	Studied the leaching of silica from the bauxite ores by individual bacteria as well as in co-operation. Mixed culture leached more silica from the solution in comparison to the individual.
Khan et al. [188]				Synthesized silica nanoparticles from fly ash by using fungus <i>F. oxysporum</i> . The purity of the biologically synthesized silica was up to 40% only with more than 50% as carbon
Fulekar and Yadav [50]	Incubation at required temperatures	<i>F. oxysporum</i> : oxalic acid <i>B. circulans</i> —EPS, MPS		Synthesized amorphous 30–80 nm, aggregated, clustered silica nanoparticles using <i>F. oxysporum</i> supernatant and sodium silicate from fly ash Synthesized amorphous 60–120 nm porous nanosheets by using <i>B. circulans</i> supernatant and sodium silicate from fly ash

7.3. Properties and Applications of SiNPs

SiNPs have always been light for their use in the field of research, industries and medicine owing to their innumerable technological and biomedical applications. SiNPs are specifically used for resins, silica-based catalysts, molecular sieves and several other materials [195]. Until now,

their application has been most exploited in biology and medicine as drug carriers [196]. Recently, biocompatible [197], bio conjugated [198] and doped SiNPs [199] have gained huge attention in cancer therapy— i.e., cancer cell imaging [200,201], DNA and microarray detection [202], barcoding tags separation [203], drug delivery [204] medicine [205] and the purification of biological molecules and cells [196]. Bulk silica is a conventional adsorbent that has been used for a very long time to remove odor. However, nowadays SiNPs have replaced conventional bulk silica and is used as a conventional adsorbent for wastewater treatment—i.e., purification of wastewater [206], removal of pollutants inorganic (heavy metals), organic pollutants (pesticides) and ultrasensitive single bacterium detection [207]. Their compounds and composites in the form of zeolites are also used for water purification.

8. Role of Nanotechnology: Nano adsorbents for Heavy Metal Removal

Nanotechnology involves the understanding and control of objects with dimensions ranging between 1–100 nm [208]. Nanotechnology is the science and art of matter that is manipulated on an atomic and molecular scale. According to the national nanotechnology initiative (NNI), nanotechnology was defined as “anything smaller than 100 nm with novel properties” [209]. The important features of nanotechnology and nanoparticles are attributed to their shape, size, surface characteristics and surface energy. As the nanoparticles have infinite size, the surface area is relatively large and consequently has higher reactivity and sorption capacity in comparison to several heavy metals [210]. These nanotechnology-based features allow the nanoparticles to become chemically more reactive by changing its strength and other properties. Hence, concerning the fortification of the environment, nanotechnology embraces the assurance of providing new and inimitable improvements [211]. Nanoparticles are used in several fields viz. wastewater treatment [212], medicine for drug delivery, electronics [213], etc. In wastewater treatment, nanoparticles are used as an adsorbents (activated carbon, silica gel, and alumina), which are generally obtained from the commercial precursors of respective nanoparticles that make them expensive, thereby making the whole adsorption mechanism cost intensive.

However, the production of the nanoadsorbents from waste materials, such as red mud [214], fly ash [215] and rice husk [216,217], makes them significantly cheaper, greener and environmentally-friendly. However, cost analysis, easy availability, non-toxicity and recyclable nature are important factors for the selection of an adsorbent for the wastewater treatment and heavy metal removal that control the total expenditure of the adsorption process. If adsorbents are derived from the waste, such as fly ash, then the adsorbent cost will definitely be low and, ultimately, so will the cost of the adsorption process. Thus, nanoparticles synthesized from waste, such as fly ash, bauxite rice husk, etc., may act as potential candidates as precursors for nanoadsorbents. Nanoparticles may serve as an efficient adsorbent for the removal of heavy metals from wastewater due to their high surface area, enhanced adsorption sites and the functional groups that are present on their surface [213]. Nanomaterials have a wide range of applications regarding the technological and environmental challenges for wastewater treatments. Numerous works have been reported based on metal oxides, as they are very effective and efficient adsorbents in the clean-up of environmental contaminants [218–220] owing to their small size, which permits them to penetrate into the contamination zone [221,222] where other bulk adsorbents and micro particles cannot.

Though the fly ash derived nanoparticles have immense potential as nanosorbents for the remediation of heavy metals from wastewater, very few works are available where such nanoparticles derived from fly ash have been used for the remediation of pollutants or heavy metals. Thus, here several examples have been provided where IONPs and SiNPs have been used for the remediation of heavy metals. Out of both IONPs and SiNPs, the former has numerous advantages over SiNPs, as it can be easily manipulated under the influence of an external magnetic field and can exhibit superparamagnetism [223–226]. Moreover, due to the presence of unpaired electrons in their 3D shell, they have Fe^{2+} , Fe^{3+} ions, and form either ferrimagnetic or ferromagnetic particles [227,228].

The magnetic properties make their recovery very easy at the end of the reaction, and they are recyclable and lower in cost. In general, IONPs exist in various forms (magnetite, maghemite, and hematite) [229–231] which are commonly used for the remediation of heavy metals from wastewater. These IONPs remediate heavy metals by adsorption techniques, which is one of the most effective techniques in comparison to precipitation [232,233], coagulation [232–234], chemical reduction [235,236], ion exchange [235,237,238] and low expenditure. Some of the examples where IONPs have been applied, for the wastewater-based remediation of heavy metals, are cited below.

Chang et al. synthesized monodisperse chitosan-coated magnetite nanoparticles with the average size of 13.5 nm and utilized them for the remediation of Cu^{2+} ions. Cu^{2+} removal efficiency was above pH 2 [235]. Yantasee et al. [239] synthesized magnetite, functionalized with thiol, with a size of 40 nm, and applied it for the remediation of Hg, Ag, Pb, and Cd. Similarly, Song et al. [240] used ($\gamma\text{-Fe}_2\text{O}_3$) encapsulated with polyrhodamine for the removal of Mn^{2+} , Cr^{2+} , Cd^{2+} , Hg^{2+} — here heavy metals were removed from the aqueous solution and it was concluded that the solution pH, initial metal ion concentration, contact time and species of metal ions influence the uptake of heavy metal ions. Chou and Lien., (2010) applied dendrimer-conjugated magnetite nanoparticles for the remediation of Zn at acidic and alkaline pHs [241]. Predescu and Nicole., (2012) synthesized and used 10 nm maghemite nanoparticles for the remediation of Zn, Cu and Cd at 2.54 pH from wastewater by adsorption [242]. Better adsorption capacity was obtained for metal ions, especially in the case of maghemite, into the cationic resin ($\gamma\text{-Fe}_2\text{O}_3\text{-R-H}$), and a higher adsorption tendency for hexavalent chromium in comparison to other metal ions. From the above work, it was concluded that, in all the cases, capped magnetic nanoparticles were synthesized from the iron precursors and further applied for the heavy metal removal.

In comparison to IONPs, SiNPs are used to a much lesser extent for the remediation of heavy metals from wastewater. They are mainly used for providing support to the nanoadsorbents or as a carrier for them. A few examples are given below where the investigators used silica either in bulk form or powder form for the removal of heavy metals, dyes, and pesticides from wastewater. Some of the selective works, cited below, focuses on the remediation of heavy metals from wastewater using SiNPs. Sheet et al. performed a study where nanosized graphite oxide, silica/graphite oxide composites and SiNPs were applied for heavy metal ion remediation from aqueous solutions using a batch adsorption method [243]. The nanosized graphene oxide-based remediation of heavy metals was in the following order: nickel>zinc>lead>cadmium>chromium. The results suggested that the optimum efficiency for heavy metal remediation is when the adsorbents (silica/graphite oxide composite) are in the ratio of (2:3). Karnib et al. comparatively studied the remediation of Cd, Pb, Zn, Cr, and Ni in a batch experiment by using activated [A_c] carbon, SiNPs and a composite of silica- A_c carbon. Ni exhibited the maximum removal percentage by A_c -Carbon at all concentrations, whereas the percentage removal reduced with an increase in the concentration of heavy metals [244]. Kong et al. reported the selective removal of heavy metals (Pb^{2+} , Cu^{2+} , Hg^{2+} , Cd^{2+} , and Zn^{2+}) from the aqueous solutions using silica fume waste-derived SiNPs with different functional groups on their surface [245].

Yadav and Fulekar 2018 reported the biogenic synthesis of IONPs from iron precursors (salts of ferrous sulphate heptahydrate and ferric chloride), by the co-precipitation method. Here, all the solutions were prepared in the aqueous leaf extract of *Tridax spp.*, which was used as a capping agent for IONPs. The synthesized IONPs were further characterized by sophisticated instruments. The synthesized IONPs ranged between 15–60 nm and were spherical in shape, but they also showed higher aggregation. The XRD and Raman revealed the mixed phases—i.e., magnetite and maghemite in the IONPs. Finally, the synthesized IONPs were used for the remediation of Pb and Cr from the 20% fly ash aqueous solutions in a batch experiment at fixed, temperature, pH, and dosage. The removal efficiency of Pb and Cr was up to 85 and 96%, respectively [21].

Yadav et al., 2020, reported the synthesis of 18–60 nm amorphous IONPs by using sonochemical methods, which were characterized by the sophisticated instruments and assessed their potential for

the remediation of fly ash heavy metals—mainly Pb and Cd in a batch adsorption study. The Pb and Cr ions were remediated up to 97.96% and 82.8%, respectively, from 20% fly ash aqueous solutions [246].

9. Conclusions

Fly ash is considered as one of the major pollutants and one million tonnes is produced every year around the globe. The disposal of fly ash into ash ponds requires a huge amount of land that, in turn, leads to water and soil pollution. Additionally, fly ash is loaded with several toxic heavy metals, which impose a potential threat to living organisms. At present, in developing countries, such as India, where the utilization rate of fly ash is only 40–50% in the form of bricks, types of cement, tiles, etc., half of the fly ash remains unutilized every year. Fly ash is rich in ferrous, alumina and silica and can be successfully used in the recovery of valuable minerals which not only reduces the pollution but also provides an alternative source for ferrous, alumina and silica for the industries. Therefore, in the present review, emphasis has been given to the advancement in the methods for the recovery of ferrous, silica and alumina nanoparticles with the latest technology and instruments. Fly ash is a spherical-shaped particle constituting elements like Al, Si, and have either Mg or Ca, S on their surface, as revealed by the EDS. The ferrous particles are generally spherical in shape, whose sizes vary between nanometers to several microns. The magnetic fractions are easily extracted by the magnetic separation method. Among non-ferrous materials—i.e., silica and alumina—they comprise major fractions of fly ash. Silica, being insoluble in acids, was preferably extracted with alkali by chemical method and microbial synthesis using *F. oxysporum* and *Bacillus spp.*. These microbes produce specific proteins and enzymes that initially leach the Si into the aqueous medium and bio transform the SiNPs. Alumina in fly ash is present in crystalline form, so it is relatively inert. Al, being amphoteric, reacts with both strong alkali and mineral acids and leaches out Al into the solution, which is processed further for the synthesis of alumina nanoparticles by chemical and microbial methods. From all the above-reported methods, the Al extraction efficiency varied between 82.5%–92.2%; it was observed that the molarity of the acids and base and temperature play an important role. The high molarity of either acids or base at high temperature may increase the yield from the fly ash. Fly ash may serve as a potential, reliable and alternative material for the ferrous-, alumina- and silica-based industries. Fly ash, deriving such nanoparticles, find reliable applications in wastewater treatment and environmental clean-up. In the future, fly ash derived nanoparticles can be used in the fields of electronics, ceramics, glass foundries, drug delivery, and agriculture, and in food industries, based on their purity.

Author Contributions: Conceptualization, design, drafting, writing, analysis and editing, V.K.Y.; Design, suggestion, analysis and editing, M.H.F. All authors have read and agreed to the published version of the manuscript.

Funding: This research received no external funding.

Conflicts of Interest: The authors declare no conflict of interest.

References

1. Choudhary, N.; Yadav, V.K.; Malik, P.; Khan, S.H.; Inwati, G.K.; Suriyaprabha, R.; Singh, B.; Yadav, A.K.; Ravi, R.K. Recovery of Natural Nanostructured Minerals: Ferrospheres, Plerospheres, Cenospheres, and Carbonaceous Particles From Fly Ash. In *Handbook of Research on Emerging Developments and Environmental Impacts of Ecological Chemistry*; Gheorghe, D., Ashok, V., Eds.; IGI Global: Hershey, PA, USA, 2020; pp. 450–470. [[CrossRef](#)]
2. Ohenoja, K.; Pesonen, J.; Yliniemi, J.; Illikainen, M. Utilization of Fly Ashes from Fluidized Bed Combustion: A Review. *Sustainability* **2020**, *12*, 2988. [[CrossRef](#)]
3. Fuller, A.; Maier, J.; Karampinis, E.; Kalivodova, J.; Grammelis, P.; Kakaras, E.; Scheffknecht, G. Fly Ash Formation and Characteristics from (co-)Combustion of an Herbaceous Biomass and a Greek Lignite (Low-Rank Coal) in a Pulverized Fuel Pilot-Scale Test Facility. *Energies* **2018**, *11*, 1581. [[CrossRef](#)]
4. Wei, Q.; Song, W. Mineralogical and Chemical Characteristics of Coal Ashes from Two High-Sulfur Coal-Fired Power Plants in Wuhai, Inner Mongolia, China. *Minerals* **2020**, *10*, 323. [[CrossRef](#)]

5. Rodrigues, P.; Silvestre, J.D.; Flores-Colen, I.; Viegas, C.A.; Ahmed, H.H.; Kurda, R.; de Brito, J. Evaluation of the Ecotoxicological Potential of Fly Ash and Recycled Concrete Aggregates Use in Concrete. *Appl. Sci.* **2020**, *10*, 351. [[CrossRef](#)]
6. Alam, J.; Akhtar, M. Fly ash utilization in different sectors in Indian scenario. *Int. J. Emerg. Trends Eng. Dev.* **2011**, *1*, 1–14.
7. Yadav, V.K.; Fulekar, M.H. The current scenario of thermal power plants and fly ash: Production and utilization with a focus in India. *Int. J. Adv. Eng. Res. Dev.* **2018**, *5*, 768–777.
8. Nisham, K.; Sridhar, M.B.; Kumar, V. Experimental study on class F fly ash cement bricks using partial replacement of fly ash by metakaolin. *Int. J. Chem. Sci.* **2016**, *14*, 227–234.
9. Yadav, V.K.; Pandita, P.R. Fly Ash Properties and Their Applications as a Soil Ameliorant. In *Amelioration Technology for Soil Sustainability*; Rathoure, A.K., Ed.; IGI Global: Hershey, PA, USA, 2019; pp. 59–89. [[CrossRef](#)]
10. Yadav, V.K.; Choudhary, N. *An Introduction to Fly Ash: Natural Nanostructured Materials*; Educreation: New Delhi, India, 2019; Volume 1, p. 162.
11. Zhao, Y.; Soltani, A.; Taheri, A.; Karakus, M.; Deng, A. Application of Slag—Cement and Fly Ash for Strength Development in Cemented Paste Backfills. *Minerals* **2018**, *9*, 22. [[CrossRef](#)]
12. Valentim, B.; Białecka, B.; Gonçalves, A.P.; Guedes, A.; Guimarães, R.; Cruceru, M.; Całus-Moszek, J.; Popescu, G.L.; Predeanu, G.; Santos, C.A. Undifferentiated Inorganics in Coal Fly Ash and Bottom Ash: Calcispheres, Magnesiocalcispheres, and Magnesiaspheres. *Minerals* **2018**, *8*, 140. [[CrossRef](#)]
13. Li, S.; Qin, S.; Kang, L.; Liu, J.; Wang, J.; Li, Y. An Efficient Approach for Lithium and Aluminum Recovery from Coal Fly Ash by Pre-Desilication and Intensified Acid Leaching Processes. *Metals* **2017**, *7*, 272. [[CrossRef](#)]
14. Habte, L.; Shiferaw, N.; Mulatu, D.; Thenepalli, T.; Chilakala, R.; Ahn, J. Synthesis of Nano-Calcium Oxide from Waste Eggshell by Sol-Gel Method. *Sustainability* **2019**, *11*, 3196. [[CrossRef](#)]
15. Peng, X. Dynamic hydrothermal synthesis of xonotlite fibers by alkali silica extraction of fly ash. *J. Eng. Fibers Fabr.* **2019**, *14*, 155892501989034. [[CrossRef](#)]
16. Purnomo, C.; Wirawan, S.; Hinode, H. The utilization of bagasse fly ash for mesoporous silica synthesis. *IOP Conf. Ser. Mater. Sci. Eng.* **2019**, *543*, 012040. [[CrossRef](#)]
17. Guo, C.; Zou, J.; Ma, S.; Yang, J.; Wang, K. Alumina Extraction from Coal Fly Ash via Low-Temperature Potassium Bisulfate Calcination. *Minerals* **2019**, *9*, 585. [[CrossRef](#)]
18. Gong, Y.; Sun, J.; Sun, S.-Y.; Lu, G.; Zhang, T.-A. Enhanced Desilication of High Alumina Fly Ash by Combining Physical and Chemical Activation. *Metals* **2019**, *9*, 411. [[CrossRef](#)]
19. Ibrahim, M.; El-Naas, M.; Benamor, A.; Al-Sobhi, S.; Zhang, Z. Carbon Mineralization by Reaction with Steel-Making Waste: A Review. *Processes* **2019**, *7*, 115. [[CrossRef](#)]
20. Valeev, D.; Mikhailova, A.; Atmadzhidi, A. Kinetics of Iron Extraction from Coal Fly Ash by Hydrochloric Acid Leaching. *Metals* **2018**, *8*, 533. [[CrossRef](#)]
21. Yadav, V.K.; Fulekar, M.H. Biogenic synthesis of maghemite nanoparticles ($\gamma\text{-Fe}_2\text{O}_3$) using Tridax leaf extract and its application for removal of fly ash heavy metals (Pb, Cd). *Mater. Today Proc.* **2018**, *5*, 20704–20710. [[CrossRef](#)]
22. Yao, Z.; Xia, M.S.; Sarker, P.; Chen, T. A review of the alumina recovery from coal fly ash, with a focus in China. *Fuel* **2014**, *120*, 74–85. [[CrossRef](#)]
23. Miricioiu, M.G.; Niculescu, V.C. Fly Ash, from Recycling to Potential Raw Material for Mesoporous Silica Synthesis. *Nanomaterials (Basel)* **2020**, *10*, 474. [[CrossRef](#)]
24. Sahoo, P.K.; Kim, K.; Powell, M.A.; Equeenuddin, S.M. Recovery of metals and other beneficial products from coal fly ash: A sustainable approach for fly ash management. *Int. J. Coal Sci. Technol.* **2016**, *3*, 267–283. [[CrossRef](#)]
25. Langmann, B. Volcanic Ash versus Mineral Dust: Atmospheric Processing and Environmental and Climate Impacts. *ISRN Atmos. Sci.* **2013**, *2013*, 17. [[CrossRef](#)]
26. Sunjidmaa, D.; Batdemberel, G.; Takibai, S. A Study of Ferrospheres in the Coal Fly Ash. *Open J. Appl. Sci.* **2019**, *9*, 10–16. [[CrossRef](#)]
27. Murugesan, S.; Ramaswamy, J.; Parshwanath, R.; Sundararaj, J.; Jose, R. Evaluation of Suitability of Alumino-Silicate Precursor for Geopolymerization through Advance Analytical Techniques. *Asian J. Chem.* **2018**, *30*, 1771–1776. [[CrossRef](#)]

28. Valentim, B.; Flores, D.; Guedes, A.; Shreya, N.; Paul, B.; Ward, C.R. Notes on the occurrence of char plerospheres in fly ashes derived from Bokaro and Jharia coals (Jharkhand, India) and the influence of the combustion conditions on their genesis. *Int. J. Coal Geol.* **2016**, *158*, 29–43. [[CrossRef](#)]
29. Salah, N.; Al-Ghamdi, A.; Memic, A.; Habib, S.; Khan, Z. Formation of Carbon Nanotubes from Carbon Rich Fly Ash: Growth Parameters and Mechanism. *Mater. Manuf. Process.* **2015**, *31*, 150811005209005. [[CrossRef](#)]
30. Silva, L.; Martinello, K.; Mardon, S.; Hower, J.; Serra-Rodríguez, C. Fullerenes and Metallofullerenes in Coal-Fired Stoker Fly Ash. *Coal Combust. Gasif. Prod.* **2010**, *2*. [[CrossRef](#)]
31. Fu, B.; Hower, J.C.; Dai, S.; Mardon, S.M.; Liu, G. Determination of Chemical Speciation of Arsenic and Selenium in High-As Coal Combustion Ash by X-ray Photoelectron Spectroscopy: Examples from a Kentucky Stoker Ash. *ACS Omega* **2018**, *3*, 17637–17645. [[CrossRef](#)]
32. Yoriya, S.; Intana, T.; Tepsri, P. Separation of Cenospheres from Lignite Fly Ash Using Acetone-Water Mixture. *Appl. Sci.* **2019**, *9*, 3792. [[CrossRef](#)]
33. Choo, T.F.; Salleh, M.A.M.; Kok, K.Y.; Matori, K.A.; Rashid, S.A. Effect of Temperature on Morphology, Phase Transformations and Thermal Expansions of Coal Fly Ash Cenospheres. *Crystals* **2020**, *10*, 481. [[CrossRef](#)]
34. Hower, J.; Groppo, J.; Graham, U.; Ward, C.; Kostova, I.; Maroto-Valer, M.; Dai, S. Coal-derived unburned carbons in fly ash: A review. *Int. J. Coal Geol.* **2017**, *179*, 11–27. [[CrossRef](#)]
35. Bayukov, O.A.; Anshits, N.N.; Balaev, A.D.; Sharonova, O.M.; Rabchevskii, E.V.; Petrov, M.I.; Anshits, A.G. Mössbauer study of magnetic microspheres isolated from power plant fly ash. *Inorg. Mater.* **2005**, *41*, 50–59. [[CrossRef](#)]
36. Wang, P.; Massoudi, M. Slag Behavior in Gasifiers. Part I: Influence of Coal Properties and Gasification Conditions. *Energies* **2013**, *6*, 784–806. [[CrossRef](#)]
37. Krishnamoorthy, V.; Pisupati, S. A Critical Review of Mineral Matter Related Issues during Gasification of Coal in Fixed, Fluidized, and Entrained Flow Gasifiers. *Energies* **2015**, *8*, 10430–10463. [[CrossRef](#)]
38. Wang, Y.-S.; Alrefaei, Y.; Dai, J.-G. Silico-Aluminophosphate and Alkali-Aluminosilicate Geopolymers: A Comparative Review. *Front. Mater.* **2019**, *6*, 106. [[CrossRef](#)]
39. Liu, H.; Sun, Q.; Wang, B.; Wang, P.; Zou, J. Morphology and Composition of Microspheres in Fly Ash from the Luohuang Power Plant, Chongqing, Southwestern China. *Minerals* **2016**, *6*, 30. [[CrossRef](#)]
40. Sharonova, O.; Anshits, N.; Fedorchak, M.; Zhizhaev, A.; Anshits, A. Characterization of Ferrospheres Recovered from High-Calcium Fly Ash. *Energy Fuels* **2015**, *29*, 5404–5414. [[CrossRef](#)]
41. Veranth, J.M.; Fletcher, T.H.; Pershing, D.W.; Sarofim, A.F. Measurement of soot and char in pulverized coal fly ash. *Fuel* **2000**, *79*, 1067–1075. [[CrossRef](#)]
42. Vassilev, S.; Menendez, R.; Borrego, A.; Díaz-Somoano, M.; Martínez-Tarazona, M. Phase-mineral and chemical composition of coal fly ashes as a basis for their multicomponent utilization. 3. Characterization of magnetic and char concentrates. *Fuel* **2004**, *83*, 1563–1583. [[CrossRef](#)]
43. Gupta, D.K.; Rai, U.N.; Tripathi, R.D.; Inouhe, M. Impacts of fly-ash on soil and plant responses. *J. Plant Res.* **2002**, *115*, 401–409. [[CrossRef](#)]
44. Singh, G.B.; Subramaniam, K.V. Characterization of Indian fly ashes using different Experimental Techniques. *Indian Concr. J.* **2018**, *92*, 10–23.
45. Šešlija, M.; Rosić, A.; Radović, N.; Vasić, M.; Đogo, M.; Jotić, M. Physiproperties of fly ash and slag from the power plants. *Geol. Croat.* **2016**, *69*, 317–324. [[CrossRef](#)]
46. Eisele, T.C.; Kawatra, S.K.; Nofal, A. Comparison of class C and class F fly-ashes as foundry sand binders and the effectiveness of accelerators in reducing curing time. *Miner. Process. Extr. Metall. Rev.* **2004**, *25*, 269–278. [[CrossRef](#)]
47. Vassilev, S.; Menendez, R.; Alvarez, D.; Díaz-Somoano, M.; Martínez-Tarazona, M. Phase-Mineral and Chemical Composition of Coal Fly Ashes as a Basis for Their Multicomponent Utilization. 1. Characterization of Feed Coals and Fly Ashes. *Fuel* **2003**, *82*, 1793–1811. [[CrossRef](#)]
48. Basu, M.; Pande, M.; Bhadoria, P.B.S.; Mahapatra, S.C. Potential fly-ash utilization in agriculture: A global review. *Prog. Nat. Sci.* **2009**, *19*, 1173–1186. [[CrossRef](#)]
49. Fulekar, M.H.; Dave, J.M. Heavy metals release from ash pond to soil water environment: A simulated technique. *Environ. Int.* **1992**, *18*, 283–295. [[CrossRef](#)]
50. Fulekar, M.H.; Yadav, V.K. Method for Separation of Ferrous, Alumina and Silica from Fly Ash. 201721035720, 7 October 2017.

51. Papatzani, S.; Paine, K. A Step by Step Methodology for Building Sustainable Cementitious Matrices. *Appl. Sci.* **2020**, *10*, 2955. [[CrossRef](#)]
52. Davison, R.L.; Natusch, D.F.; Wallace, J.R.; Evans, C.A., Jr. Trace elements in fly ash. Dependence of concentration on particle size. *Environ. Sci. Technol.* **1974**, *8*, 1107–1113. [[CrossRef](#)]
53. Boboc, V.; Rotaru, A.; Boboc, A. A material for substructure and road works: Mechanical characteristics of pozzolana fly ash from thermal power plant of Iasi, Romania. *WSEAS Trans. Environ. Dev.* **2010**, *42*, 437–446.
54. Yunusa, I.; Loganathan, P.; Nissanka, S.; Veeragathipillai, M.; Burchett, M.; Skilbeck, C.; Eamus, D. Application of Coal Fly Ash in Agriculture: A Strategic Perspective. *Crit. Rev. Environ. Sci. Technol.* **2012**, *42*, 559–600. [[CrossRef](#)]
55. Kleinhans, U.; Wieland, C.; Frandsen, F.J.; Spliethoff, H. Ash formation and deposition in coal and biomass fired combustion systems: Progress and challenges in the field of ash particle sticking and rebound behavior. *Prog. Energy Combust. Sci.* **2018**, *68*, 65–168. [[CrossRef](#)]
56. Wuana, R.A.; Okieimen, F.E. Heavy Metals in Contaminated Soils: A Review of Sources, Chemistry, Risks and Best Available Strategies for Remediation. *ISRN Ecol.* **2011**, *2011*, 20. [[CrossRef](#)]
57. Fulekar, M.H.; Naik, D.S.; Dave, J.M. Heavy metals in Indian coals and corresponding fly-ash and their relationship with particulate size. *Int. J. Environ. Stud.* **1983**, *21*, 179–182. [[CrossRef](#)]
58. Chou, M.-I.M. Fly Ash. In *Encyclopedia of Sustainability Science and Technology*; Meyers, R.A., Ed.; Springer: New York, NY, USA, 2012; pp. 3820–3843. [[CrossRef](#)]
59. Ngu, L.-N.; Wu, H.; Zhang, D.-k. Characterization of Ash Cenospheres in Fly Ash from Australian Power Stations. *Energy Fuels* **2007**, *21*, 3437–3445. [[CrossRef](#)]
60. Żyrkowski, M.; Neto, R.C.; Santos, L.; Witkowski, K. Characterization of fly-ash cenospheres from coal-fired power plant unit. *Fuel* **2016**, *174*, 49–53. [[CrossRef](#)]
61. Fisher, G.L.; Chang, D.P.Y.; Brummer, M. Fly Ash Collected from Electrostatic Precipitators: Microcrystalline Structures and the Mystery of the Spheres. *Science* **1976**, *192*, 553–555. [[CrossRef](#)]
62. Zhao, Y.; Zhang, J.; Sun, J.; Bai, X.; Zheng, C. Mineralogy, Chemical Composition, and Microstructure of Ferrospheres in Fly Ashes from Coal Combustion. *Energy Fuels* **2006**, *20*, 1490–1497. [[CrossRef](#)]
63. Ibeto, C.N.; Obiefuna, C.J.; Ugwu, K.E. Environmental effects of concretes produced from partial replacement of cement and sand with coal ash. *Int. J. Environ. Sci. Technol.* **2020**, *17*, 2967–2976. [[CrossRef](#)]
64. Meer, I.; Nazir, R. Removal techniques for heavy metals from fly ash. *J. Mater. Cycles Waste Manag.* **2017**, *20*, 703–722. [[CrossRef](#)]
65. Zhang, W.; Noble, A.; Yang, X.; Honaker, R. A Comprehensive Review of Rare Earth Elements Recovery from Coal-Related Materials. *Minerals* **2020**, *10*, 451. [[CrossRef](#)]
66. Kunecki, P.; Panek, R.; Wdowin, M.; Bień, T.; Franus, W. Influence of the fly ash fraction after grinding process on the hydrothermal synthesis efficiency of Na-A, Na-Pl, Na-X and sodalite zeolite types. *Int. J. Coal Sci. Technol.* **2020**. [[CrossRef](#)]
67. Kishor, P.; Ghosh, A.; Kumar, D. Use of Flyash in Agriculture: A Way to Improve Soil Fertility and its Productivity. *Asian J. Agric. Res.* **2010**, *4*, 1–14. [[CrossRef](#)]
68. Singh, R.P.; Gupta, A.K.; Ibrahim, M.H.; Mittal, A.K. Coal fly ash utilization in agriculture: Its potential benefits and risks. *Rev. Environ. Sci. Bio/Technol.* **2010**, *9*, 345–358. [[CrossRef](#)]
69. Behera, A.; Mohapatra, S.S. Challenges in Recovery of Valuable and Hazardous Elements from Bulk Fly Ash and Options for Increasing Fly Ash Utilization. In *Coal Fly Ash Beneficiation—Treatment of Acid Mine Drainage with Coal Fly Ash*; Akinyemi, S., Gitari, M.W., Eds.; IntechOpen: London, UK, 2018; pp. 19–39. [[CrossRef](#)]
70. Attarde, S.; Marathe, S.; Sil, A. Utilization of fly ash in construction industries for environment management. *Int. J. Environ. Sci.* **2014**, *3*, 117–121.
71. Luo, Y.; Zheng, S.; Ma, S.; Liu, C.; Wang, X. Ceramic tiles derived from coal fly ash: Preparation and mechanical characterization. *Ceram. Int.* **2017**, *43*, 11953–11966. [[CrossRef](#)]
72. FİGen, A.; ÖZÇay, Ü.; Pişkin, S. Manufacturing and Characterization of Roof Tiles a Mixture of Tile Waste and Coal Fly Ash. *Süleyman Demirel Üniversitesi Fen Bilimleri Enstitüsü Derg.* **2017**, *21*, 10. [[CrossRef](#)]
73. Zhuang, X.Y.; Chen, L.; Komarneni, S.; Zhou, C.H.; Tong, D.S.; Yang, H.M.; Yu, W.H.; Wang, H. Fly ash-based geopolymer: Clean production, properties and applications. *J. Clean. Prod.* **2016**, *125*, 253–267. [[CrossRef](#)]
74. Nordin, N.; Abdullah, M.M.A.B.; Tahir, M.F.M.; Sandu, A.V.; Hussin, K. Utilization of fly ash waste as construction material. *Int. J. Conserv. Sci.* **2016**, *7*, 161–166.

75. Tyson, S.; Blackstock, T. Coal combustion fly ash—Overview of applications and opportunities in the USA. *Fuel Energy Abstr.* **1996**, *37*, 422.
76. Martin, J.; Collins, R.; Browning, J.; Bichl, J. Properties and Use of Fly Ashes for Embankments. *J. Energy Eng.* **1990**, *116*, 71–86. [[CrossRef](#)]
77. Baykal, G.; Edinçliler, A.; Saygılı, A. Highway embankment construction using fly ash in cold regions. *Resour. Conserv. Recycl.* **2004**, *42*, 209–222. [[CrossRef](#)]
78. Dasgupta, M.; Kar, S.; Gupta, S.D.; Mukhopadhyay, R.; Bandyopadhyay, A. Effect of Fly Ash as Filler in Rubber—A Comprehensive Study of the Vulcanisate Properties of Styrene-Butadiene Rubber Compounds. *Prog. Rubber Plast. Recycl. Technol.* **2013**, *29*, 151–168. [[CrossRef](#)]
79. Gaikwad, A.; Patel, B.K.; Verma, V.; Rai, A. Development of fly ash based new Bio-Composites Material as Wood Substitute. *Int. J. Mech. Prod. Eng. Res. Dev.* **2017**, *7*, 1–6.
80. Nadesan, M.S.; Dinakar, P. Mix design and properties of fly ash waste lightweight aggregates in structural lightweight concrete. *Case Stud. Constr. Mater.* **2017**, *7*, 336–347. [[CrossRef](#)]
81. Rudić, O.; Ducman, V.; Malešev, M.; Radonjanin, V.; Draganić, S.; Šupić, S.; Radeka, M. Aggregates Obtained by Alkali Activation of Fly Ash: The Effect of Granulation, Pelletization Methods and Curing Regimes. *Materials* **2019**, *12*, 776. [[CrossRef](#)]
82. Valeev, D.; Kunilova, I.; Alpatov, A.; Varnavskaya, A.; Ju, D. Magnetite and Carbon Extraction from Coal Fly Ash Using Magnetic Separation and Flotation Methods. *Minerals* **2019**, *9*, 320. [[CrossRef](#)]
83. Brännvall, E.; Kumpiene, J. Fly ash in landfill top covers—A review. *Environ. Sci. Process. Impacts* **2016**, *18*, 11–21. [[CrossRef](#)]
84. Ahmed, S.; Saurikhia, A.; Haleem, A.; Gangopadhyay, S. Geographical spread of fly ash generation and residual potential for its utilization in India. *Int. J. Innov. Res. Rev.* **2016**, *4*, 8–19.
85. Namkane, K.; Naksata, W.; Thiansem, S.; Sooksamiti, P.; Arqueropanyo, O.-A. Utilization of coal bottom ash as raw material for production of ceramic floor tiles. *Environ. Earth Sci.* **2016**, *75*, 386. [[CrossRef](#)]
86. Dwivedi, A.; Jain, M. Fly ash—Waste management and overview: A Review. *Recent Res. Sci. Technol.* **2014**, *6*, 30–35.
87. Ghosal, S.; Self, S.A. Particle size-density relation and cenosphere content of coal fly ash. *Fuel* **1995**, *74*, 522–529. [[CrossRef](#)]
88. Amin, N.U. A multi-directional utilization of different ashes. *RSC Adv.* **2014**, *4*, 62769–62788. [[CrossRef](#)]
89. Suriyanarayanan, N.; Nithin, K.K.; Bernardo, E. Mullite glass ceramics production from coal fly ash and alumina by high temperature plasma. *J. Non-Oxide Glasses* **2009**, *1*, 247–260.
90. Zhao, Y.; Zhang, J.; Tian, C.; Li, H.; Shao, X.; Zheng, C. Mineralogy and Chemical Composition of High-Calcium Fly Ashes and Density Fractions from a Coal-Fired Power Plant in China. *Energy Fuels* **2010**, *24*, 834–843. [[CrossRef](#)]
91. Kutchko, B.G.; Kim, A.G. Fly ash characterization by SEM–EDS. *Fuel* **2006**, *85*, 2537–2544. [[CrossRef](#)]
92. Ashrafi, F. Synthesis of alumina nano powder using sol-gel method and chelate precursor. *Asian Acad. Res. J. Multidiscip.* **2015**, *2*, 2319–2801.
93. Song, X.L.; Qu, P.; Yang, H.P.; He, X.; Qiu, G.Z. Synthesis of γ -Al₂O₃ nanoparticles by chemical precipitation method. *J. Cent. South Univ. Technol.* **2005**, *12*, 536–541. [[CrossRef](#)]
94. Narayanan, M.V.; Rakesh, S.G. Synthesis of colloidal alumina nanoparticles using green method. *IOP Conf. Ser. Mater. Sci. Eng.* **2018**, *402*, 1–9. [[CrossRef](#)]
95. Itskos, G.; Koutsianos, A.; Koukouzas, N.; Vasilatos, C. Zeolite development from fly ash and utilization in lignite mine-water treatment. *Int. J. Miner. Process.* **2015**, *139*, 43–50. [[CrossRef](#)]
96. Park, H.C.; Park, Y.J.; Stevens, R. Synthesis of alumina from high purity alum derived from coal fly ash. *Mater. Sci. Eng. A* **2004**, *367*, 166–170. [[CrossRef](#)]
97. Liang, G.; Li, Y.; Yang, C.; Zi, C.; Zhang, Y.; Hu, X.; Zhao, W. Production of biosilica nanoparticles from biomass power plant fly ash. *Waste Manag.* **2020**, *105*, 8–17. [[CrossRef](#)] [[PubMed](#)]
98. Kgabi, N.A.; Waanders, F.B.; Taole, S.H. Iron-Sulphur Compounds of South African Coal. *Eur. J. Sci. Res.* **2009**, *34*, 190–195.
99. Xie, P.; Song, H.; Wei, J.; Li, Q. Mineralogical Characteristics of Late Permian Coals from the Yueliangtian Coal Mine, Guizhou, Southwestern China. *Minerals* **2016**, *6*, 29. [[CrossRef](#)]
100. Waanders, F.; Vinken, E.; Mans, A.; Mulaba-Bafubandi, A. Iron Minerals in Coal, Weathered Coal and Coal Ash—SEM and Mössbauer Results. *Hyperfine Interact.* **2003**, *148–149*, 21–29. [[CrossRef](#)]

101. Biggs, D.L.; Lindsay, C.G. High-Temperature Interactions among Minerals Occurring in Coal. In *Mineral Matter and Ash in Coal*; American Chemical Society: Washington, DC, USA, 1986; Volume 301, pp. 128–137.
102. Waanders, F.B.; Mohamed, W.; Wagner, N.J. Changes of pyrite and pyrrhotite in coal upon microwave treatment. *J. Phys. Conf. Ser.* **2010**, *217*, 012051. [[CrossRef](#)]
103. Cohn, C.A.; Laffers, R.; Simon, S.R.; O’Riordan, T.; Schoonen, M.A.A. Role of pyrite in formation of hydroxyl radicals in coal: Possible implications for human health. *Part. Fibre Toxicol.* **2006**, *3*, 10. [[CrossRef](#)]
104. de Aldecoa, A.L.; Roldan, F.V.; Menor-Salvan, C. Natural pyrrhotite as a catalyst in prebiotic chemical evolution. *Life* **2013**, *3*, 502–517. [[CrossRef](#)]
105. Querol, X.; Alastuey, A.; Chinchon, J.S.; Turiel, J.F.; Soler, A.L. Determination of pyritic sulphur and organic matter contents in Spanish subbituminous coals by X-ray power diffraction. *Int. J. Coal Geol.* **1993**, *22*, 279–293. [[CrossRef](#)]
106. Laita, E.; Bauluz, B.; Yuste, A. High-Temperature Mineral Phases Generated in Natural Clinkers by Spontaneous Combustion of Coal. *Minerals* **2019**, *9*, 213. [[CrossRef](#)]
107. Yuan, Y.; Tang, S.; Zhang, S. Geochemical and Mineralogical Characteristics of the Middle Jurassic Coals from the Tongjialiang Mine in the Northern Datong Coalfield, Shanxi Province, China. *Minerals* **2019**, *9*, 184. [[CrossRef](#)]
108. Spears, D.A.; Caswell, S.A. Mineral matter in coals: Cleat minerals and their origin in some coals from the english midlands. *Int. J. Coal Geol.* **1986**, *6*, 107–125. [[CrossRef](#)]
109. Lin, Z.; Li, P.; Hou, D.; Kuang, Y.; Wang, G. Aggregation Mechanism of Particles: Effect of Ca²⁺ and Polyacrylamide on Coagulation and Flocculation of Coal Slime Water Containing Illite. *Minerals* **2017**, *7*, 30. [[CrossRef](#)]
110. Giménez-García, R.; Vigil de la Villa Mencía, R.; Rubio, V.; Frías, M. The Transformation of Coal-Mining Waste Minerals in the Pozzolan Reactions of Cements. *Minerals* **2016**, *6*, 64. [[CrossRef](#)]
111. Kholodov, V.N.; Butuzova, G.Y. Siderite formation and evolution of sedimentary iron ore deposition in the Earth’s history. *Geol. Ore Depos.* **2008**, *50*, 299. [[CrossRef](#)]
112. O’Brien, G.; Firth, B.; Adair, B. The Application of the Coal Grain Analysis Method to Coal Liberation Studies. *Int. J. Coal Prep. Util.* **2011**, *31*, 96–111. [[CrossRef](#)]
113. Sokol, E.; Kalugin, V.; Nigmatulina, E.N.; Volkova, N.; Frenkel, A.E.; Maksimova, N.V. Ferrospheres from fly ashes of Chelyabinsk coals: Chemical composition, morphology and formation conditions. *Fuel* **2002**, *81*, 867–876. [[CrossRef](#)]
114. Yamaura, M.; Fungaro, D.A. Synthesis and characterization of magnetic adsorbent prepared by magnetite nanoparticles and zeolite from coal fly ash. *J. Mater. Sci.* **2013**, *48*, 5093–5101. [[CrossRef](#)]
115. Lu, S.G.; Chen, Y.Y.; Shan, H.D.; Bai, S.Q. Mineralogy and heavy metal leachability of magnetic fractions separated from some Chinese coal fly ashes. *J. Hazard. Mater.* **2009**, *169*, 246–255. [[CrossRef](#)]
116. Joseph, A.; Snellings, R.; Van den Heede, P.; Matthys, S.; De Belie, N. The Use of Municipal Solid Waste Incineration Ash in Various Building Materials: A Belgian Point of View. *Materials* **2018**, *11*, 141. [[CrossRef](#)]
117. Bayukov, O.A.; Anshits, N.N.; Balaev, A.D.; Sharonova, O.M.; Petrov, M.I.; Rabchevskii, E.V.; Anshits, A.G. Mossbauer and magnetic study of microspheres extracted from fly ashes of power stations. *Phys. Met. Metallogr.* **2006**, *102*, S53–S56. [[CrossRef](#)]
118. Shoumkova, A.S. Magnetic separation of coal fly ash from Bulgarian power plants. *Waste Manag. Res.* **2010**, *29*, 1078–1089. [[CrossRef](#)] [[PubMed](#)]
119. Shoumkova, A.S. Physico-chemical characterization and magnetic separation of coal fly ashes from “varna”, “bobov Dol” and “maritza- Istok” power plants, Bulgaria, i—Physico-chemical characteristics. *J. Univ. Chem. Technol. Metall.* **2006**, *41*, 175–180.
120. Xue, Q.-F.; Lu, S.-G. Microstructure of ferrospheres in fly ashes: SEM, EDX and ESEM analysis. *J. Zhejiang Univ. Sci. A Appl. Phys. Eng.* **2008**, *9*, 1595–1600. [[CrossRef](#)]
121. Oliveira, M.; Marostega, F.; Taffarel, S.; Saikia, B.K.; Waanders, F.; Martinello, K.; Baruah, B.P.; Silva, L. Nano-mineralogical investigation of coal and fly ashes from coal-based captive power plant (India): An introduction of occupational health hazards. *Sci. Total Environ.* **2013**, *468–469*, 1128–1137. [[CrossRef](#)]
122. Fomenko, E.V.; Anshits, N.N.; Kushnerova, O.A.; Akimochkina, G.V.; Kukhtetskiy, S.V.; Anshits, A.G. Separation of Nonmagnetic Fine Narrow Fractions of PM10 from Coal Fly Ash and Their Characteristics and Mineral Precursors. *Energy Fuels* **2019**, *33*, 3584–3593. [[CrossRef](#)]

123. Devasahayam, S.; Raman, R.K.; Chennakesavulu, K.; Bhattacharya, S. Plastics—Villain or Hero? Polymers and Recycled Polymers in Mineral and Metallurgical Processing—A Review. *Materials* **2019**, *12*, 655. [[CrossRef](#)] [[PubMed](#)]
124. Vereshchagin, S.; Kondratenko, E.; Rabchevskii, E.; Anshits, N.; Solov'ev, L.A.; Anshits, A.G. New approach to the preparation of catalysts for the oxidative coupling of methane. *Kinet. Catal.* **2012**, *53*, 449–455. [[CrossRef](#)]
125. Saraswat, M.; Musante, L.; Ravidá, A.; Shortt, B.; Byrne, B.; Holthofer, H. Preparative Purification of Recombinant Proteins: Current Status and Future Trends. *BioMed Res. Int.* **2013**, *2013*, 18. [[CrossRef](#)]
126. Choudhary, V.R.; Uphade, B.S.; Mulla, S.A.R. Oxidative Coupling of Methane over a Sr-Promoted La₂O₃ Catalyst Supported on a Low Surface Area Porous Catalyst Carrier. *Ind. Eng. Chem. Res.* **1997**, *36*, 3594–3601. [[CrossRef](#)]
127. Anshits, N.N.; Fedorchak, M.A.; Fomenko, E.V.; Mazurova, E.V.; Anshits, A.G. Composition, Structure, and Formation Routes of Blocklike Ferrospheres Separated from Coal and Lignite Fly Ashes. *Energy Fuels* **2020**, *34*, 3743–3754. [[CrossRef](#)]
128. Anshits, A.G.; Bayukov, O.A.; Kondratenko, E.V.; Anshits, N.N.; Pletnev, O.N.; Rabchevskii, E.V.; Solovyov, L.A. Catalytic properties and nature of active centers of ferrospheres in oxidative coupling of methane. *Appl. Catal. A Gen.* **2016**, *524*, 192–199. [[CrossRef](#)]
129. Gomes, S.; François, M.; Abdelmoula, M.; Refait, P.; Pellissier, C.; Evrard, O. Characterization of magnetite in silico-aluminous fly ash by SEM, TEM, XRD, magnetic susceptibility, and Mössbauer spectroscopy. *Cem. Concr. Res.* **1999**, *29*, 1705–1711. [[CrossRef](#)]
130. Yadav, V.K.; Fulekar, M.H. Isolation and Characterization of Iron Nanoparticles From Coal Fly Ash From Gandhinagar (Gujarat) Thermal Power Plant (A Mechanical Method of Isolation). *Int. J. Eng. Res. Technol.* **2014**, *3*, 471–479.
131. Orwat, K.; Bernard, P.; Migdał-Mikuli, A. Obtaining and Investigating Amphoteric Properties of Aluminum Oxide in a Hands-On Laboratory Experiment for High School Students. *J. Chem. Educ.* **2016**, *93*, 906–909. [[CrossRef](#)]
132. Kelmers, A.D.; Canon, R.M.; Egan, B.Z.; Felker, L.K.; Gilliam, T.M.; Jones, G.; Owen, G.D.; Seeley, F.G.; Watson, J.S. Chemistry of the direct acid leach, calciner, and pressure digestion-acid leach methods for the recovery of alumina from fly ash. *Resour. Conserv.* **1982**, *9*, 271–279. [[CrossRef](#)]
133. Jung, J.; Park, H.; Stevens, R. Mullite ceramics derived from coal fly ash. *J. Mater. Sci. Lett.* **2001**, *20*, 1089–1091. [[CrossRef](#)]
134. Dos Santos, R.P.; Martins, J.; Gadelha, C.; Cavada, B.; Albertini, A.V.; Arruda, F.; Vasconcelos, M.; Teixeira, E.; Alves, F.; Filho, J.L.; et al. Coal fly ash ceramics: Preparation, characterization, and use in the hydrolysis of sucrose. *Sci. World J.* **2014**, 1–7. [[CrossRef](#)]
135. Liu, N.; Peng, J.; Zhang, L.; Wang, S.; Huang, S.; He, S. Extraction of Aluminum from Coal Fly Ash by Alkali Activation with Microwave Heating. *J. Residuals Sci. Technol.* **2016**, *13*, S181–S187. [[CrossRef](#)]
136. Su, S.Q.; Yang, J.; Ma, H.W.; Jiang, F.; Liu, Y.Q.; Li, G. Preparation of Ultrafine Aluminum Hydroxide from Coal Fly Ash by Alkali Dissolution Process. *Integr. Ferroelectr.* **2011**, *128*, 155–162. [[CrossRef](#)]
137. Li, H.; Hui, J.; Wang, C.; Bao, W.; Sun, Z. Extraction of alumina from coal fly ash by mixed-alkaline hydrothermal method. *Hydrometallurgy* **2014**, *147–148*, 183–187. [[CrossRef](#)]
138. Matjie, R.H.; Bunt, J.R.; van Heerden, J.H.P. Extraction of alumina from coal fly ash generated from a selected low rank bituminous South African coal. *Miner. Eng.* **2005**, *18*, 299–310. [[CrossRef](#)]
139. Qin, J.; Gu, S. Process for Recovery of Silica Followed by Alumina from Coal Fly Ash. U.S. Patent 7,871,583, 18 January 2011.
140. Rampou, M.; Ndlovu, S.; Shemi, A. Purification of Coal Fly Ash Leach Liquor for Alumina Recovery Using an Integrated Precipitation and Solvent Extraction Process. *J. Sustain. Metall.* **2017**, *3*, 782–792. [[CrossRef](#)]
141. Boudreault, R.; Fournier, J.; Dumont, H.; Samuel, J.F.; Bouffard, J.; Lepage, S.; Huard, A.C.; Gravel-Rouleau, C.; Labrecque-Gilbert, M.M. Methods for Purifying Aluminium Ions. U.S. Patent 9,534,274, 3 January 2017.
142. Sibanda, V.; Ndlovu, S.; Dombo, G.; Shemi, A.; Rampou, M. Towards the Utilization of Fly Ash as a Feedstock for Smelter Grade Alumina Production: A Review of the Developments. *J. Sustain. Metall.* **2016**, *2*, 167–184. [[CrossRef](#)]
143. Sun, Y.; Liang, Z.; Sun, F. Recovery of Alumina from Coal Fly Ash by CaCl₂ Calcination Followed by H₂SO₄ Leaching. *J. Environ. Anal. Toxicol.* **2017**, *7*, 1–6. [[CrossRef](#)]

144. Wang, R.-C.; Zhai, Y.-C.; Ning, Z.-Q. Thermodynamics and kinetics of alumina extraction from fly ash using an ammonium hydrogen sulfate roasting method. *Int. J. Miner. Metall. Mater.* **2014**, *21*, 144–149. [[CrossRef](#)]
145. Park, J.; Son, Y.; Noh, S.; Bong, T. An Evaluation of the Environmental Safety and Geochemical Characteristics of Coal Combustion Products. *KSCE J. Civ. Eng.* **2017**, *22*, 1–9. [[CrossRef](#)]
146. Wang, R.-C.; Zhai, Y.-C.; Wu, X.-W.; Ning, Z.-Q.; Pei, H. Extraction of alumina from fly ash by ammonium hydrogen sulfate roasting technology. *Trans. Nonferr. Met. Soc. China* **2014**, *24*, 1596–1603. [[CrossRef](#)]
147. Nayak, N.; Panda, C. Aluminium extraction and leaching characteristics of Talcher Thermal Power Station fly ash with sulphuric acid. *Fuel* **2010**, *89*, 53–58. [[CrossRef](#)]
148. Li, L.S.; Wu, Y.S.; Liu, Y.Y.; Zhai, Y.C. Extraction of alumina from coal fly ash with sulfuric acid leaching method. *Chin. J. Process Eng.* **2011**, *11*, 255–258.
149. Shi, Z.; Bonneville, S.C.; Krom, M.; Carslaw, K.; Jickells, T.; Baker, A.; Benning, L. Iron dissolution kinetics of mineral dust at low pH during simulated atmospheric processing. *Atmos. Chem. Phys.* **2011**, *11*, 995–1007. [[CrossRef](#)]
150. Bai, G.; Teng, W.; Wang, X.; Zhang, H.; Xu, P. Processing and kinetics studies on the alumina enrichment of coal fly ash by fractionating silicon dioxide as nano particles. *Fuel Process. Technol.* **2010**, *91*, 175–184. [[CrossRef](#)]
151. Wu, C.; Yu, H.-F.; Zhang, H.-F. Extraction of aluminum by pressure acid-leaching method from coal fly ash. *Trans. Nonferr. Met. Soc. China* **2012**, *22*, 2282–2288. [[CrossRef](#)]
152. Shemi, A.; Ndlovu, S.; Sibanda, V.; van Dyk, L. Extraction of alumina from coal fly ash using an acid leach-sinter-acid leach technique. *Hydrometallurgy* **2015**, *157*, 348–355. [[CrossRef](#)]
153. Valeev, D.; Shoppert, A.; Mikhailova, A.; Kondratiev, A. Acid and Acid-Alkali Treatment Methods of Al-Chloride Solution Obtained by the Leaching of Coal Fly Ash to Produce Sandy Grade Alumina. *Metals* **2020**, *10*, 585. [[CrossRef](#)]
154. Das, A.; Mishra, A.K. Role of Thiobacillus ferrooxidans and sulphur (sulphide)-dependent ferric-ion-reducing activity in the oxidation of sulphide minerals. *Appl. Microbiol. Biotechnol.* **1996**, *45*, 377–382. [[CrossRef](#)]
155. Wang, R.; Lin, J.-Q.; Liu, X.-M.; Pang, X.; Zhang, C.-J.; Yang, C.-L.; Gao, X.-Y.; Lin, C.-M.; Li, Y.-Q.; Li, Y.; et al. Sulfur Oxidation in the Acidophilic Autotrophic *Acidithiobacillus* spp. *Front. Microbiol.* **2019**, *9*, 3290. [[CrossRef](#)] [[PubMed](#)]
156. Ferreira, P.; Servulo, E.; da Costa, A.C.; Ferreira, D.; Godoy, M.; Oliveira, F. Bioleaching of metals from a spent diesel hydrodesulfurization catalyst employing *Acidithiobacillus thiooxidans* FG-01. *Braz. J. Chem. Eng.* **2017**, *34*, 119–129. [[CrossRef](#)]
157. Koschorreck, M. Microbial sulphate reduction at a low pH. *FEMS Microbiol. Ecol.* **2008**, *64*, 329–342. [[CrossRef](#)]
158. Kimura, S.; Johnson, D. Sulfidogenesis in Low pH (3.8–4.2) Media by a Mixed Population of Acidophilic Bacteria. *Biodegradation* **2006**, *17*, 159–167. [[CrossRef](#)]
159. Monrroy, M.; Rueda, L.; Aparicio, A.; García, J. Fermentation of *Musa paradisica* Peels to Produce Citric Acid. *J. Chem.* **2019**, *2019*, 1–8. [[CrossRef](#)]
160. Ferreira-Guedes, S.; Mendes, B.; Leitão, A.L. Degradation of 2,4-dichlorophenoxyacetic acid by a halotolerant strain of *Penicillium chrysogenum*: Antibiotic production. *Environ. Technol.* **2012**, *33*, 677–686. [[CrossRef](#)] [[PubMed](#)]
161. Bazgha, A.; Haq, N.B.; Sadia, I. Bio-extraction of metal ions from laterite ore by *Penicillium chrysogenum*. *Afr. J. Biotechnol.* **2011**, *10*, 11196–11205. [[CrossRef](#)]
162. Bosshard, P.P.; Bachofen, R.; Brandl, H. Metal Leaching of Fly Ash from Municipal Waste Incineration by *Aspergillus niger*. *Environ. Sci. Technol.* **1996**, *30*, 3066–3070. [[CrossRef](#)]
163. Khan, A.H.; Karuppaiyil, S.M. Fungal pollution of indoor environments and its management. *Saudi J. Biol. Sci.* **2012**, *19*, 405–426. [[CrossRef](#)]
164. Vachon, P.; Tyagi, R.D.; Auclair, J.C.; Wilkinson, K.J. Chemical and biological leaching of aluminum from red mud. *Environ. Sci. Technol.* **1994**, *28*, 26–30. [[CrossRef](#)] [[PubMed](#)]
165. Xu, T.-J.; Ting, Y.-P. Optimisation on bioleaching of incinerator fly ash by *Aspergillus niger*—Use of central composite design. *Enzym. Microb. Technol.* **2004**, *35*, 444–454. [[CrossRef](#)]
166. Xu, T.-J.; Ramanathan, T.; Ting, Y.-P. Bioleaching of incineration fly ash by *Aspergillus niger*—Precipitation of metallic salt crystals and morphological alteration of the fungus. *Biotechnol. Rep.* **2014**, *3*, 8–14. [[CrossRef](#)]
167. Xu, T.-J.; Ting, Y.-P. Fungal bioleaching of incineration fly ash: Metal extraction and modeling growth kinetics. *Enzym. Microb. Technol. Enzym. Microb. Technol.* **2009**, *44*, 323–328. [[CrossRef](#)]

168. Krishna, P.; Babu, A.G.; Reddy, M.S. Bacterial diversity of extremely alkaline bauxite residue site of alumina industrial plant using culturable bacteria and residue 16S rRNA gene clones. *Extremophiles* **2014**, *18*, 665–676. [[CrossRef](#)]
169. Argyle, M.; Bartholomew, C. Heterogeneous Catalyst Deactivation and Regeneration: A Review. *Catalysts* **2015**, *5*, 145–269. [[CrossRef](#)]
170. Hassanpour, P.; Panahi, Y.; Ebrahimi-Kalan, A.; Akbarzadeh, A.; Davaran, S.; Nasibova, A.N.; Khalilov, R.; Kavetsky, T. Biomedical applications of aluminium oxide nanoparticles. *Micro Nano Lett.* **2018**, *13*, 1227–1231. [[CrossRef](#)]
171. Hakuta, Y.; Nagai, N.; Suzuki, Y.H.; Kodaira, T.; Bando, K.K.; Takashima, H.; Mizukami, F. Preparation of α -alumina nanoparticles with various shapes via hydrothermal phase transformation under supercritical water conditions. *IOP Conf. Ser. Mater. Sci. Eng.* **2013**, *47*, 012045. [[CrossRef](#)]
172. Daimatsu, K.; Sugimoto, H.; Kato, Y.; Nakanishi, E.; Inomata, K.; Amekawa, Y.; Kazuki, T. Preparation and physical properties of flame retardant acrylic resin containing nano-sized aluminum hydroxide. *Polym. Degrad. Stab.* **2007**, *92*, 1433–1438. [[CrossRef](#)]
173. Suchanek, W.L. Hydrothermal Synthesis of Alpha Alumina (α -Al₂O₃) Powders: Study of the Processing Variables and Growth Mechanisms. *J. Am. Ceram. Soc.* **2010**, *93*, 399–412. [[CrossRef](#)]
174. Matori, K.A.; Wah, L.C.; Hashim, M.; Ismail, I.; Zaid, M.H.M. Phase Transformations of α -Alumina Made from Waste Aluminum via a Precipitation Technique. *Int. J. Mol. Sci.* **2012**, *13*, 16812–16821. [[CrossRef](#)]
175. Ilyas, S.; Pendyala, R.; Marneni, N. Settling Characteristics of Alumina Nanoparticles in Ethanol-Water Mixtures. *Appl. Mech. Mater.* **2013**, *372*, 143–148. [[CrossRef](#)]
176. Tang, Y.; Chen, F.L. Extracting alumina from fly ash by soda lime sintering method. *Min. Metall. Eng.* **2008**, *28*, 73–75.
177. Zhu, P.-W.; Dai, H.; Han, L.; Xu, X.-L.; Cheng, L.-M.; Wang, Q.-H.; Shi, Z.-L. Aluminum extraction from coal ash by a two-step acid leaching method. *J. Zhejiang Univ. Sci. A* **2015**, *16*, 161–169. [[CrossRef](#)]
178. Zhang, Y.; Dong, J.; Guo, F.; Shao, Z.; Wu, J. Zeolite Synthesized from Coal Fly Ash Produced by a Gasification Process for Ni²⁺ Removal from Water. *Minerals* **2018**, *8*, 116. [[CrossRef](#)]
179. Chaudhary, S.; Banerjee, D.K. Speciation of some heavy metals in coal fly ash. *Chem. Speciat. Bioavailab.* **2015**, *19*, 95–102. [[CrossRef](#)]
180. Falayi, T.; Okonta, F.N.; Ntuli, F. Desilication of fly ash and development of lightweight construction blocks from alkaline activated desilicated fly ash. *Int. J. Environ. Waste Manag.* **2017**, *20*, 233–253. [[CrossRef](#)]
181. Piekos, R.; Paslawska, S. Leaching characteristics of flouride from coal fly ash. *Digit. Arch. Fluoride J.* **1988**, *31*, 188–192.
182. Yadav, V.K.; Fulekar, M.H. Green synthesis and characterization of amorphous silica nanoparticles from fly ash. *Mater. Today Proc.* **2019**, *18*, 4351–4359. [[CrossRef](#)]
183. Adnan, M.; Shah, Z.; Fahad, S.; Arif, M.; Alam, M.; Khan, I.A.; Mian, I.A.; Basir, A.; Ullah, H.; Arshad, M.; et al. Phosphate-Solubilizing Bacteria Nullify the Antagonistic Effect of Soil Calcification on Bioavailability of Phosphorus in Alkaline Soils. *Sci. Rep.* **2017**, *7*, 16131. [[CrossRef](#)] [[PubMed](#)]
184. Kang, S.-M.; Waqas, M.; Shahzad, R.; You, Y.-H.; Asaf, S.; Khan, M.A.; Lee, K.-E.; Joo, G.-J.; Kim, S.-J.; Lee, I.-J. Isolation and characterization of a novel silicate-solubilizing bacterial strain Burkholderia eburnea CS4-2 that promotes growth of japonica rice (*Oryza sativa* L. cv. Dongjin). *Soil Sci. Plant Nutr.* **2017**, *63*, 233–241. [[CrossRef](#)]
185. Wang, Z.; Xu, G.; Ma, P.; Lin, Y.; Yang, X.; Cao, C. Isolation and Characterization of a Phosphorus-Solubilizing Bacterium from Rhizosphere Soils and Its Colonization of Chinese Cabbage (*Brassica campestris* ssp. chinensis). *Front. Microbiol.* **2017**, *8*, 1270. [[CrossRef](#)]
186. Janczura, E.; Perkins, H.R.; Rogers, H.J. Teichuronic acid: A mucopolysaccharide present in wall preparations from vegetative cells of *Bacillus subtilis*. *Biochem. J.* **1961**, *80*, 82–93. [[CrossRef](#)]
187. Zhan, S.; Liu, J.; Chen, Y.; Sun, D. Single and Cooperative Bauxite Bioleaching by Silicate Bacteria. *Ieri Procedia* **2013**, *5*, 172–177. [[CrossRef](#)]
188. Khan, S.A.; Uddin, I.; Moez, S.; Ahmad, A. Fungus-Mediated Preferential Bioleaching of Waste Material Such as Fly—Ash as a Means of Producing Extracellular, Protein Capped, Fluorescent and Water Soluble Silica Nanoparticles. *PLoS ONE* **2014**, *9*, e0107597. [[CrossRef](#)]
189. Nakamura, L.K.; Swezey, J. Taxonomy of *Bacillus circulans* Jordan 1890: Base Composition and Reassociation of Deoxyribonucleic Acid. *Int. J. Syst. Evol. Microbiol.* **1983**, *33*, 46–52. [[CrossRef](#)]

190. Gadd, G.M. Metals, minerals and microbes: Geomicrobiology and bioremediation. *Microbiology* **2009**, *156*, 609–643. [[CrossRef](#)] [[PubMed](#)]
191. Bahira, S.; Raut, S.; Sharma, D. Bioleaching of Alumina from low grade Indian bauxite (41% Al₂O₃) by indigenous bacteria with reference to pH, Time and Carbon source. *Int. Res. J. Environ. Sci.* **2018**, *7*, 20–27.
192. Vrvic, M.; Matić, V.; Vučetić, J.; Vitorović, D. Demineralization of an oil shale by *Bacillus circulans* ("siliceous bacteria"). *Org. Geochem.* **1990**, *16*, 1203–1209. [[CrossRef](#)]
193. Savostin, P. Microbial transformation of silicates. *Z. Für Pflanz. Und Bodenkd.* **1972**, *132*, 37–45. [[CrossRef](#)]
194. Groudev, S. Biobeneficiation of mineral raw material. In *Mineral Biotechnology: Microbial Aspects of Mineral Beneficiation, Metal Extraction, and Environmental Control*; Kawatra, S.K., Natarajan, K.A., Eds.; Society for Mining, Metallurgy, and Exploration: Englewood, CO, USA, 2001; Volume 16, pp. 37–54.
195. Li, C.; Wang, X.; Jiao, Z.; Zhang, Y.; Yin, X.; Cui, X.; Wei, Y. Functionalized Porous Silica-Based Nano/Micro Particles for Environmental Remediation of Hazard Ions. *Nanomaterials* **2019**, *9*, 247. [[CrossRef](#)]
196. Salata, O.V. Applications of nanoparticles in biology and medicine. *J. Nanobiotechnol.* **2004**, *2*, 1–6. [[CrossRef](#)]
197. Asefa, T.; Tao, Z. Biocompatibility of Mesoporous Silica Nanoparticles. *Chem. Res. Toxicol.* **2012**, *25*, 2265–2284. [[CrossRef](#)]
198. Wang, L.; Zhao, W.; Tan, W. Bioconjugated Silica Nanoparticles: Development and Applications. *Nano Res.* **2008**, *1*, 99–115. [[CrossRef](#)]
199. Bae, S.W.; Tan, W.; Hong, J.-I. Fluorescent dye-doped silica nanoparticles: New tools for bioapplications. *Chem. Commun.* **2012**, *48*, 2270–2282. [[CrossRef](#)]
200. Luigi, P.; Antonella, L.; Diego, S.; Sebastiano, A.; Catia, M. Mesoporous Silica Nanoparticles in Cancer Therapy: Relevance of the Targeting Function. *Mini-Rev. Med. Chem.* **2016**, *16*, 743–753. [[CrossRef](#)]
201. Rosenholm, J.; Mamaeva, V.; Sahlgren, C.; Lindén, M. Nanoparticles in targeted cancer therapy: Mesoporous silica nanoparticles entering preclinical development stage. *Nanomed. (Lond. Engl.)* **2012**, *7*, 111–120. [[CrossRef](#)] [[PubMed](#)]
202. Enrichi, F.; Ricco, R.; Meneghello, A.; Pierobon, R.; Canton, G.; Cretaio, E. Enhancing the Sensitivity of DNA Microarray Using Dye-Doped Silica Nanoparticles: Detection of Human Papilloma Virus. In *AIP Conference Proceedings*; American Institute of Physics: College Park, MD, USA, 2010; Volume 1275, pp. 154–157.
203. Wang, L.; Tan, W. Multicolor FRET silica nanoparticles by single wavelength excitation. *Nano Lett.* **2006**, *6*, 84–88. [[CrossRef](#)]
204. Bharti, C.; Nagaich, U.; Pal, A.K.; Gulati, N. Mesoporous silica nanoparticles in target drug delivery system: A review. *Int. J. Pharm. Investig.* **2015**, *5*, 124–133. [[CrossRef](#)] [[PubMed](#)]
205. O'Farrell, N.; Houlton, A.; Horrocks, B.R. Silicon nanoparticles: Applications in cell biology and medicine. *Int. J. Nanomed.* **2006**, *1*, 451–472. [[CrossRef](#)]
206. Ahmad, I.Z.; Ahmad, A.; Tabassum, H.; Kuddus, M. Applications of Nanoparticles in the Treatment of Wastewater. In *Handbook of Ecomaterials*; Martínez, L.M.T., Kharissova, O.V., Kharisov, B.I., Eds.; Springer International Publishing: Cham, Switzerland, 2019; pp. 275–299. [[CrossRef](#)]
207. Zhao, W.; Wang, L.; Tan, W. Fluorescent Nanoparticle for Bacteria and DNA Detection. In *Bio-Applications of Nanoparticles*; Chan, W.C.W., Ed.; Springer: New York, NY, USA, 2007; pp. 129–135. [[CrossRef](#)]
208. Chitra, K.; Annadurai, G. Fluorescent Silica Nanoparticles in the Detection and Control of the Growth of Pathogen. *J. Nanotechnol.* **2013**, *2013*, 7. [[CrossRef](#)]
209. Khan, I.; Saeed, K.; Khan, I. Nanoparticles: Properties, applications and toxicities. *Arab. J. Chem.* **2019**, *12*, 908–931. [[CrossRef](#)]
210. Lu, H.; Wang, J.; Stoller, M.; Wang, T.; Bao, Y.; Hao, H. An Overview of Nanomaterials for Water and Wastewater Treatment. *Adv. Mater. Sci. Eng.* **2016**, *2016*, 10. [[CrossRef](#)]
211. Mishra, S.; Keswani, C.; Abhilash, P.C.; Fraceto, L.F.; Singh, H.B. Integrated Approach of Agri-nanotechnology: Challenges and Future Trends. *Front. Plant Sci.* **2017**, *8*, 471. [[CrossRef](#)]
212. Kaushal, A.; Singh, S. Removal of heavy metals by nanoadsorbents: A review. *J. Environ. Biotechnol. Res.* **2017**, *6*, 96–104.
213. Agarwal, P.; Gupta, R.; Agarwal, N. Advances in Synthesis and Applications of Microalgal Nanoparticles for Wastewater Treatment. *J. Nanotechnol.* **2019**, *2019*, 9. [[CrossRef](#)]
214. Dong, W.; Liang, K.; Qin, Y.; Ma, H.; Zhao, X.; Zhang, L.; Zhu, S.; Yu, Y.; Bian, D.; Yang, J. Hydrothermal Conversion of Red Mud into Magnetic Adsorbent for Effective Adsorption of Zn(II) in Water. *Appl. Sci.* **2019**, *9*, 1519. [[CrossRef](#)]

215. Ge, J.; Yoon, S.; Choi, N. Application of Fly Ash as an Adsorbent for Removal of Air and Water Pollutants. *Appl. Sci.* **2018**, *8*, 1116. [[CrossRef](#)]
216. Ahmaruzzaman, M.; Gupta, V.K. Rice Husk and Its Ash as Low-Cost Adsorbents in Water and Wastewater Treatment. *Ind. Eng. Chem. Res.* **2011**, *50*, 13589–13613. [[CrossRef](#)]
217. Pham, T.; Bui, T.; Nguyen, V.; Bui, T.; Tran, T.; Phan, Q.; Pham, T.; Hoang, T. Adsorption of Polyelectrolyte onto Nanosilica Synthesized from Rice Husk: Characteristics, Mechanisms, and Application for Antibiotic Removal. *Polymers* **2018**, *10*, 220. [[CrossRef](#)] [[PubMed](#)]
218. Plohl, O.; Finšgar, M.; Gyergyek, S.; Ajdnik, U.; Ban, I.; Zemljič, L.F. Efficient Copper Removal from an Aqueous Environment using a Novel and Hybrid Nano-adsorbent Based on Derived-Polyethyleneimine Linked to Silica Magnetic Nanocomposites. *Nanomaterials* **2019**, *9*, 209. [[CrossRef](#)] [[PubMed](#)]
219. Wang, Z.; Wu, A.; Ciacchi, L.C.; Wei, G. Recent Advances in Nanoporous Membranes for Water Purification. *Nanomaterials* **2018**, *8*, 65. [[CrossRef](#)]
220. Guerra, F.; Attia, M.; Whitehead, D.; Alexis, F. Nanotechnology for Environmental Remediation: Materials and Applications. *Molecules* **2018**, *23*, 1760. [[CrossRef](#)]
221. Ray, P.C.; Yu, H.; Fu, P.P. Toxicity and Environmental Risks of Nanomaterials: Challenges and Future Needs. *J. Environ. Sci. Health Part C* **2009**, *27*, 1–35. [[CrossRef](#)] [[PubMed](#)]
222. Khin, M.M.; Nair, A.S.; Babu, V.J.; Murugan, R.; Ramakrishna, S. A review on nanomaterials for environmental remediation. *Energy Environ. Sci.* **2012**, *5*, 8075–8109. [[CrossRef](#)]
223. Singh, N.; Sallem, F.; Mirjole, C.; Nury, T.; Sahoo, S.K.; Millot, N.; Kumar, R. Polydopamine Modified Superparamagnetic Iron Oxide Nanoparticles as Multifunctional Nanocarrier for Targeted Prostate Cancer Treatment. *Nanomaterials* **2019**, *9*, 138. [[CrossRef](#)]
224. Pham, B.; Colvin, E.; Pham, N.; Kim, B.; Fuller, E.; Moon, E.; Barbey, R.; Yuen, S.; Rickman, B.; Bryce, N.; et al. Biodistribution and Clearance of Stable Superparamagnetic Maghemite Iron Oxide Nanoparticles in Mice Following Intraperitoneal Administration. *Int. J. Mol. Sci.* **2018**, *19*, 205. [[CrossRef](#)] [[PubMed](#)]
225. Arias, L.; Pessan, J.; Vieira, A.; Lima, T.; Delbem, A.; Monteiro, D. Iron Oxide Nanoparticles for Biomedical Applications: A Perspective on Synthesis, Drugs, Antimicrobial Activity, and Toxicity. *Antibiotics* **2018**, *7*, 46. [[CrossRef](#)] [[PubMed](#)]
226. Fernández-Barahona, I.; Muñoz-Hernando, M.; Herranz, F. Microwave-Driven Synthesis of Iron-Oxide Nanoparticles for Molecular Imaging. *Molecules* **2019**, *24*, 1224. [[CrossRef](#)]
227. Maity, D.; Agrawal, D. Synthesis of Iron Oxide Nanoparticles under Oxidizing Environment and Their Stabilization in Aqueous and Non-Aqueous Media. *J. Magn. Magn. Mater.* **2007**, *308*, 46–55. [[CrossRef](#)]
228. Teja, A.S.; Koh, P.-Y. Synthesis, properties, and applications of magnetic iron oxide nanoparticles. *Prog. Cryst. Growth Charact. Mater.* **2009**, *55*, 22–45. [[CrossRef](#)]
229. Saif, S.; Tahir, A.; Asim, T.; Chen, Y.; Adil, S. Polymeric Nanocomposites of Iron–Oxide Nanoparticles (IONPs) Synthesized Using Terminalia chebula Leaf Extract for Enhanced Adsorption of Arsenic (V) from Water. *Colloids Interfaces* **2019**, *3*, 17. [[CrossRef](#)]
230. Lee, Y.-H.; Zhuang, Y.-N.; Wang, H.-T.; Wei, M.-F.; Ko, W.-C.; Chang, W.-J.; Way, T.-F.; Rwei, S.-P. Fabrication of Self-Healable Magnetic Nanocomposites via Diels–Alder Click Chemistry. *Appl. Sci.* **2019**, *9*, 506. [[CrossRef](#)]
231. Dar, M.I.; Shivashankar, S.A. Single crystalline magnetite, maghemite, and hematite nanoparticles with rich coercivity. *RSC Adv.* **2014**, *4*, 4105–4113. [[CrossRef](#)]
232. Nguyen, K.; Nguyen, B.; Nguyen, H.; Nguyen, H. Adsorption of Arsenic and Heavy Metals from Solutions by Unmodified Iron-Ore Sludge. *Appl. Sci.* **2019**, *9*, 619. [[CrossRef](#)]
233. Charentanyarak, L. Heavy metals removal by chemical coagulation and precipitation. *Water Sci. Technol.* **1999**, *39*, 135–138. [[CrossRef](#)]
234. Inam, M.; Khan, R.; Park, D.; Lee, Y.-W.; Yeom, I. Removal of Sb(III) and Sb(V) by Ferric Chloride Coagulation: Implications of Fe Solubility. *Water* **2018**, *10*, 418. [[CrossRef](#)]
235. Wang, M.; Wang, Z.; Zhou, X.; Li, S. Efficient Removal of Heavy Metal Ions in Wastewater by Using a Novel Alginate-EDTA Hybrid Aerogel. *Appl. Sci.* **2019**, *9*, 547. [[CrossRef](#)]
236. Yang, J.; Hou, B.; Wang, J.; Tian, B.; Bi, J.; Wang, N.; Li, X.; Huang, X. Nanomaterials for the Removal of Heavy Metals from Wastewater. *Nanomaterials* **2019**, *9*, 424. [[CrossRef](#)]
237. Dąbrowski, A.; Hubicki, Z.; Podkościelny, P.; Robens, E. Selective removal of the heavy metal ions from waters and industrial wastewaters by ion-exchange method. *Chemosphere* **2004**, *56*, 91–106. [[CrossRef](#)] [[PubMed](#)]

238. Pan, L.; Wang, Z.; Yang, Q.; Huang, R. Efficient Removal of Lead, Copper and Cadmium Ions from Water by a Porous Calcium Alginate/Graphene Oxide Composite Aerogel. *Nanomaterials* **2018**, *8*, 957. [[CrossRef](#)] [[PubMed](#)]
239. Yantasee, W.; Warner, C.L.; Sangvanich, T.; Addleman, R.S.; Carter, T.G.; Wiacek, R.J.; Fryxell, G.E.; Timchalk, C.; Warner, M.G. Removal of Heavy Metals from Aqueous Systems with Thiol Functionalized Superparamagnetic Nanoparticles. *Environ. Sci. Technol.* **2007**, *41*, 5114–5119. [[CrossRef](#)] [[PubMed](#)]
240. Song, J.; Kong, H.; Jang, J. Adsorption of Heavy Metal Ions from Aqueous Solution by Polyrhodanine-Encapsulated Magnetic Nanoparticles. *J. Colloid Interface Sci.* **2011**, *359*, 505–511. [[CrossRef](#)]
241. Chou, C.-M.; Lien, H.-L. Dendrimer-conjugated magnetic nanoparticles for removal of zinc(II) from aqueous solutions. *J. Nanopart. Res.* **2010**, *13*, 2099–2107. [[CrossRef](#)]
242. Predescu, A.; Nicolae, A. Adsorption of Zn, Cu and Cd from waste waters by means of maghemite nanoparticles. *UPB Sci. Bull. Ser. B Chem. Mater. Sci.* **2012**, *74*, 255–264.
243. Sheet, I.; Kabbani, A.; Holail, H. Removal of Heavy Metals Using Nanostructured Graphite Oxide, Silica Nanoparticles and Silica/Graphite Oxide Composite. *Energy Procedia* **2014**, *50*, 130–138. [[CrossRef](#)]
244. Karnib, M.; Kabbani, A.; Holail, H.; Olama, Z. Heavy Metals Removal Using Activated Carbon, Silica and Silica Activated Carbon Composite. *Energy Procedia* **2014**, *50*, 113–120. [[CrossRef](#)]
245. Kong, X.; Yang, B.; Xiong, H.; Zhou, Y.; Xu, B.-Q.; Wang, S.-X. Selective removal of heavy metal ions from aqueous solutions with surface functionalized silica nanoparticles by different functional groups. *J. Cent. South Univ.* **2014**, *21*, 3575–3579. [[CrossRef](#)]
246. Yadav, V.K.; Ali, D.; Khan, S.H.; Gnanamoorthy, G.; Choudhary, N.; Yadav, K.K.; Thai, V.N.; Hussain, S.A.; Manhrdas, S. Synthesis and Characterization of Amorphous Iron Oxide Nanoparticles by the Sonochemical Method and Their Application for the Remediation of Heavy Metals from Wastewater. *Nanomaterials* **2020**, *10*, 1551. [[CrossRef](#)] [[PubMed](#)]



© 2020 by the authors. Licensee MDPI, Basel, Switzerland. This article is an open access article distributed under the terms and conditions of the Creative Commons Attribution (CC BY) license (<http://creativecommons.org/licenses/by/4.0/>).